Auger formation of the $(^3\text{He}\mu p)_J^{2+}$ molecule in collisions of muonic hydrogen $p\mu$ with helium at energies 0.1–50 eV

W. Czapliński[*]

AGH University of Science and Technology, Faculty of Physics and Applied Computer Science,
Aleja A. Mickiewicza 30, 30-059 Krakow, Poland
(Received 31 December 2012; revised manuscript received 1 August 2013; published 25 September 2013)

Results on Auger formation of the $(^3\text{He}\mu p)_J^{2+}$ molecule (and its generalization to any isotopes of hydrogen and helium) in collisions of muonic hydrogen with helium atom and ion in the ground and singly excited state are presented for all rotational states J of the molecule. The corresponding reaction rates are calculated in the energy range 0.1–50 eV using a one-level adiabatic approximation for the $2p\sigma$ state of the three-body system $^3\text{He}^{2+}$-μ-p and the dipole approximation for the interaction of the three-body system with helium electrons. It is found that reaction rates corresponding to the formation of $(^3\text{He}\mu p)_1^{2+}$, $(^4\text{He}\mu d)_2^{2+}$, and $(^{3,4}\text{He}\mu t)_2^{2+}$ molecules are significantly enhanced by shape resonances in $(h\mu)_{1s} + \text{He}^{2+}$ collisions (where $h = p,d,t$ and $\text{He}^{2+} = {}^{3,4}\text{He}^{2+}$) situated between 7 and 33 eV. In particular, reaction rates for the formation of the $(^3\text{He}\mu p)_1^{2+}$ molecule in the vicinity of the resonant energy (12.9 eV) are almost two orders of magnitude greater than those presented by Aristov *et al.* [Sov. J. Nucl. Phys. **33**, 564 (1981)]. Average reaction rates for the formation of the molecules in triple H-H′-He gas mixtures (H and H′ denote different hydrogen isotopes) at temperatures between 30 and 5000 K, as well as in H-He plasma at temperature $T \leqslant 50$ eV, are also presented. Rotational ground states of the molecules $J = 0$, from which nuclear synthesis is preferred, are considerably populated both in triple mixtures and in H-He plasma. The results may be interesting from the point of view of the experimental study of muon-catalyzed nuclear fusion.

PACS number(s): 34.50.Fa, 36.10.Ee, 52.25.Dg

I. INTRODUCTION

Negative muon μ entering a gaseous mixture of light elements initiates a complicated chain of atomic and molecular processes ending in the muon decay [1]. The most important of these processes are the formation of excited muonic atoms and their subsequent deexcitation due to radiative, Auger, and Coulomb transitions, muon transfer between atomic orbits of different elements, the formation of muonic molecular ions (usually referred to as muonic molecules) such as $(dt\mu)^+$, $(^3\text{He}\mu d)^{2+}$, $(^6\text{Li}\mu p)^{3+}$, etc., and probably the most spectacular process which is nuclear fusion occurring within these molecules. Muon freed after the fusion may initiate another chain of processes whose common designation is muon-catalyzed fusion (MCF) [2–8]. Muonic molecules are small objects, whose nuclei are separated by a distance being of the order of inverse muon mass, $1/207$ (in atomic units). The nuclei of hydrogen isotopes approach one another to this distance if their collision energy is about 3 keV [7] ($\sim$5 keV for collision of hydrogen and helium nuclei). However, such low energies are hardly reachable in accelerator experiments. Therefore, the muonic molecules provide an interesting tool for the investigation of nucleus-nucleus interactions at low energies, especially for the investigation of charge symmetry of strong interactions [9] and for the problem of the abundance of light nuclei in stars and in our galaxy [10]. At the same time, the processes in question (including spin flip in muonic atoms) form an unavoidable background in the experimental investigation of weak muon capture by hydrogen and helium nuclei [11], which provides information on such important issues as the value of a proton's pseudoscalar coupling constant

g_P [12], solar p-p fusion and neutrino-deuterium scattering [13], or the structure of light [14] and heavy atomic nuclei [15]. The observation of radiative transitions in muonic atoms as well as muon transfer from muonic hydrogen to heavier elements provides information on short-living radioisotopes [16]. The muonic helium atom $[(^4\text{He}^{2+}\mu)^+,e]$ plays a role of the heaviest hydrogen isotope ^4H and provides a unique opportunity for studies of isotopic mass effects in chemical reactions that involve hydrogen [17]. Recently, a very precise value of the root-mean-square charge radius of proton was obtained from the measurement of the Lamb shift in the $p\mu$ atom [18].

Helium nuclei unavoidably appear even in initially pure deuterium and deuterium-tritium targets exposed on a negative muon's beam: $^3\text{He}^{2+}$ is produced in the β decay of triton as well as in d-d fusion, and $^4\text{He}^{2+}$ results from d-t fusion [5–8]. If the muon becomes bound in the atomic orbit of helium (either as a result of direct capture of free muon or muon transfer from muonic hydrogen, or due to sticking to helium produced in the fusion), a positively charged ion is formed (with a large binding energy), which terminates the MCF chain. On the other hand, the presence of helium atoms enables the formation of quasistationary states $(\text{He}\mu h)_{J\upsilon}^{2+}$, called hydrogen-helium muonic molecules ($\text{He} = {}^{3,4}\text{He}$, $h = p,d,t$, whereas J and υ are rotational and vibrational quantum numbers), due to collisions of helium atoms with muonic hydrogen isotopes (the so-called Auger formation process),

$$(h\mu)_{1s} + \text{He} \rightarrow [(\text{He}\mu h)_{J0}^{2+},e]^+ + e. \tag{1a}$$
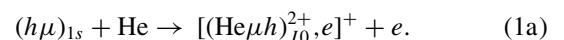
In particular, the formation of $(^3\text{He}\mu d)_{00}^{2+}$ is of special importance because nuclear fusion $^3\text{He} + d \rightarrow \alpha(3.5\text{ MeV}) + p(14.64\text{ MeV})$ occurring within this molecule releases relatively large energy without the emission of neutrons.

---
[*]gjczapli@cyf-kr.edu.pl

The hydrogen-helium muonic molecules correspond to narrow Feshbach resonances [19] in $(He\mu)_{1s}^+ + h$ scattering at about 8 keV. However, these resonant states can be formed spontaneously in process (1a). The existence of the states for $J = 0,1$ ($h = p$) and $J = 0,1,2(h = d,t)$, was theoretically predicted by Aristov *et al.* [20]. The resonances decay after about 10^{-12} s-10^{-10} s [21,22] due to the transition to the unbound $(He\mu)_{1s}^+ + h$ state via one of three processes: predissociation, radiative decays, and Auger decays:

$$[(He\mu h)_{J0}^{2+},e]^+ \rightarrow [(He\mu)_{1s}^+,e] + h \rightarrow [(He\mu)_{1s}^+,e] + h + \gamma$$
$$\rightarrow (He\mu)_{1s}^+ + h + e. \quad (1b)$$

The ground and the first excited state of the He^{2+}-μ-h system correspond asymptotically to $(He\mu)_{1s}^+ + h$ and $He^{2+} + (h\mu)_{1s}$, respectively, and are described by the respective molecular terms $1s\sigma$ and $2p\sigma$. Their asymptotic energy spacing is about 8 keV. Of these two terms, only the latter produces a potential well, which allows for the existence of quasistationary states $(He\mu h)_{J0}^{2+}$. Energy levels of the states, situated between 0.134 and 81.335 eV below $(h\mu)_{1s}$ thresholds, have been calculated quite accurately in [20,22,23] using a one-level adiabatic approximation corresponding to the $2p\sigma$ state of the three-body system He^{2+}-μ-h. In this approximation (briefly called the adiabatic approximation hereafter), the one-dimensional partial-wave equation is solved with the $2p\sigma$ adiabatic potential. Binding energies of the molecules, calculated with respect to the dissociation threshold corresponding to $He^{2+} + (h\mu)_{1s}$, are consistent (within several percent) with those obtained in Refs. [24–28] using more refined methods, i.e., the nonadiabatic coupled-rearrangement channel, the hyperspherical expansion, and the complex-coordinate rotation. Another group of resonances, i.e., shape resonances, which are supported by the attractive part of the $2p\sigma$ potential and the centrifugal potential barrier, were found in Ref. [23] using the adiabatic approximation. The resonances are situated between 7 and 33 eV above the $(h\mu)_{1s}$ threshold and correspond to partial waves $L = 2,3$ of $(h\mu)_{1s} + He^{2+}$ relative motion. They are collected in Table I.

Due to the small dimensions of the muonic molecules, which are much smaller than the dimensions of a helium atom and ion, the formation process (1a) is practically determined by the interaction of the dipole moment of the He^{++}-μ-h system with helium electrons (this approximation is briefly called the dipole approximation hereafter). The interaction results in the transition from the scattering state $(h\mu)_{1s} + He$ to the bound state $[(He\mu h)_{J0}^{2+},e]^+$. The transition energy is transferred to the outgoing helium electron. Consequently, in

room-temperature targets, the molecules are formed in the rotational state $J = 1$ due to s-wave collisions. Reaction rates (also referred to as formation rates) defined as $\lambda = N_0 v\sigma$, where $N_0 = 4.25 \times 10^{22}$ cm^{-3} is the liquid hydrogen density (LHD), v is the collision velocity, and σ is the formation cross section, have been calculated in Refs. [20,29,30] only for rotational states of the molecules $J = 1$, namely, for collision energies up to 1 eV in Refs. [29,30] and up to 20 eV in Ref. [20]. The calculations have been performed using the adiabatic and the dipole approximations. The results range between 10^7 s^{-1} and 10^9 s^{-1} and are significantly greater than reaction rates for direct muon transfer [31], i.e., occurring without the formation of the intermediate molecular state. Formation rates calculated for slow collisions, $\varepsilon \leqslant 0.4$ eV, where ε is the collision energy, are in good agreement with the rates measured experimentally in low-temperature binary hydrogen-helium mixtures [32]. At the same time, experimental results corresponding to collision energies exceeding 1 eV are not yet available. Only the s wave of $(h\mu)_{1s} + He^{2+}$ relative motion was taken into account in Refs. [20,29,30], whereas partial wave $L = 2$, also contributing to the formation of the rotational state $J = 1$, was not included. As was shown in Ref. [33], shape resonances in elastic $(p\mu)_{1s} + {}^4He^{2+}$ and $(d\mu)_{1s} + {}^3He^{2+}$ scattering for d and f partial waves at about 7 and 33 eV, respectively (see Table I), lead to a significant enhancement of the formation rates for the corresponding molecules, $({}^4He\mu p)_1^{2+}$ and $({}^3He\mu d)_2^{2+}$. [The vibrational quantum number of molecules formed due to process (1a) is generally equal to 0 and, therefore, subscript v is omitted in the following notation. The only exception is the $({}^4He\mu t)_{01}^{2+}$ molecule [25], which formation is not considered here.] The contribution of the d wave to the formation of the $({}^4He\mu p)_1^{2+}$ molecule is dominating above 1 eV and leads to reaction rates that are about one order of magnitude greater than those presented in [20] for 10 and 20 eV. One can expect, therefore, that resonances corresponding to partial waves $L = 2$ and 3 in elastic $(p\mu)_{1s} + {}^3He^{2+}$, $(d\mu)_{1s} + {}^4He^{2+}$, and $(t\mu)_{1s} + {}^{3,4}He^{2+}$ scattering will also significantly influence the reaction rates for the formation of the corresponding molecules: $({}^3He\mu p)_1^{2+}$, $({}^4He\mu d)_2^{2+}$, and $({}^{3,4}He\mu t)_2^{2+}$. In particular, it can be expected that formation rates for the first molecule will be greater than those presented in Ref. [20] in the vicinity of the corresponding resonant energy.

The analogous resonant enhancement of reaction rates corresponding to the formation of $(p\mu d)_1^+$ and $(p\mu t)_1^+$ molecules in hydrogen isotope mixtures was found in [34]. It was shown that the enhancement was caused by resonances

TABLE I. Energies ε_r and widths Γ_r of shape resonances in $(h\mu)_{1s} + He^{2+}$ scattering for partial wave L. Binding energies ε_J^b of $(He\mu h)_{J0}^{2+}$ molecules calculated relative to the ground-state level of $(h\mu)_{1s}$ are also presented. The data are taken from Ref. [23].

	^{3}He				^{4}He			
		ε_J^b (eV)				ε_J^b (eV)		
	$(\varepsilon_r,\Gamma_r)_L$ (eV)	$J = 0$	$J = 1$	$J = 2$	$(\varepsilon_r,\Gamma_r)_L$ (eV)	$J = 0$	$J = 1$	$J = 2$
p	$(12.9,6.6)_2$	67.2	34.2		$(7.4,2.0)_2$	73.85	41.6	
d	$(32.7,21.7)_3$	69.5	46.5	7.25	$(23.1,10.1)_3$	77.5	55.9	17.7
t	$(19.0,7.5)_3$	71.6	52.4	18.2	$(7.9,0.8)_3$	80.5	62.9	30.7

in elastic $(d\mu)_{1s} + p$ and $(t\mu)_{1s} + p$ scattering for partial wave $L = 2$. The resonances were found in [35] for each isotope composition of the $h\mu + h'$ system (except $p\mu + p$) for $L = 2$ and 3, using the two-level adiabatic approximation. The presence of the resonances at nearly the same collision energies was confirmed by more refined calculations [36], where several hundred terms of the adiabatic expansion for the two-center Coulomb problem were used.

In the present paper, reaction rates for the Auger formation of $(\mathrm{He}\mu h)_J^{2+}$ molecules due to collisions of $(h\mu)_{1s}$ atoms with helium atoms and ions in the ground and singly excited states,

$$(h\mu)_{1s} + \mathrm{He}^* \rightarrow \left[(\mathrm{He}\mu h)_J^{2+}, e\right]^+ + e, \qquad (2)$$

$$(h\mu)_{1s} + (\mathrm{He}^+)^* \rightarrow (\mathrm{He}\mu h)_J^{2+} + e, \qquad (3)$$
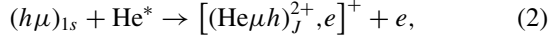
are calculated for all possible rotational states of the molecules $J = 0, 1, 2$. The rates are presented as functions of collision energy in the range 0.1–50 eV for the principal quantum number of the excited helium electron, $n \leqslant 10$. Results are obtained using the adiabatic and the dipole approximations, as well as the independent-particle model, to describe helium electrons. Average reaction rates for the formation of the molecules in triple H-D-He, H-T-He, and D-T-He gas mixtures at temperatures $T = 30$–5000 K, are calculated as functions of the kinetic energy of $(h\mu)_{1s}$ atoms formed due to muon transfer from lighter to heavier hydrogen isotope. Furthermore, Auger formation of the molecules in H-He plasma at temperatures $T \leqslant 50$ eV is also considered and the corresponding formation rates averaged over the Maxwell distribution and populations of singly excited helium atoms and ions present in the plasma are also calculated.

This paper is arranged as follows. The method of calculations is described in Sec. II, results are presented and discussed in Sec. III, and the summary and conclusions are given in Sec. IV.

II. METHOD OF CALCULATION

A. Auger formation of hydrogen-helium muonic molecules

All resonances presented in Table I are situated above 1 eV and, therefore, the electron screening in entrance channels of Auger formation (2) and (3) is neglected. At the same time, the simplest treatment of the two electrons involved in the formation (2), i.e., the independent-particle model exploiting variational and Hartree-Fock wave functions, is used. Process (2) is considered first, taking into account a possible excitation or deexcitation of the electron in the final complexes,

$$(h\mu)_{1s} + [\mathrm{He}^{2+}, e(1s)\, e(n_i l_i m_i)]$$
$$\rightarrow \left[(\mathrm{He}\mu h)_J^{2+}, e(n_f l_f m_f)\right]^+ + e, \qquad (4)$$
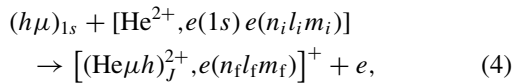
where $(n_i l_i m_i)$ and $(n_f l_f m_f)$ are spherical quantum numbers of the excited electron in the initial (i) and the final (f) state. The transition is induced by the interaction of the three-body system He^{2+}-μ-h with helium electrons. Due to small dimensions of the resulting muonic molecule, the dipole approximation for the interaction of the three-body system with electrons of helium atom and ion is justified (atomic units are used throughout unless explicitly stated),

$$V_{\mathrm{dip}} = -\mathbf{d} \cdot \boldsymbol{\mathcal{E}}, \qquad (5)$$
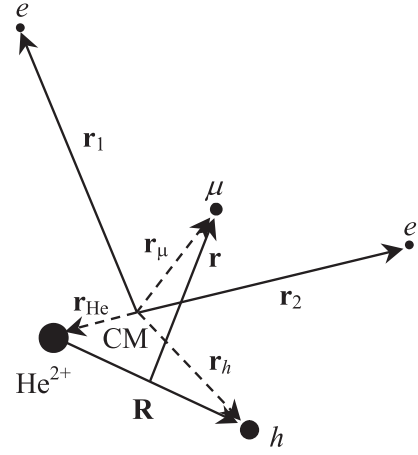
FIG. 1. Coordinates used in calculation. "CM" denotes center of mass of the three-body system He^{2+}-μ-h; vector $\mathbf{r}$ connects the midpoint of $\mathbf{R}$ with the muon.

where $\mathbf{d} = \sum_c Z_c\, \mathbf{r}_c$ is the dipole moment of the three-body system, $c = \mathrm{He}^{2+}, h, \mu$, and Z_c is the corresponding electric charge; $\boldsymbol{\mathcal{E}} = \sum_{j=1}^{2} \hat{\mathbf{r}}_j r_j^{-2}$ is the electric field formed by the two electrons at the center of mass of the three-body system; $\hat{\mathbf{r}}_j = \mathbf{r}_j/r_j$. Coordinates of the particles involved in process (4) are defined in Fig. 1.

Interaction potential (5) is considered as a perturbation and calculations are performed in the first order of perturbation theory. Formation process (4) is induced then by the dipole transition $L \rightarrow J = |L \pm 1|$, where L and J are the rotational quantum numbers of the three-body system in the initial (scattering) and the final (molecular) state, respectively. The corresponding zero-order Hamiltonian is

$$\hat{H} = \hat{H}_{3\mathrm{b}} + \hat{H}_{\mathrm{He}}, \qquad (6)$$

where terms proportional to m_e/m_c (m_e is electron mass), which couple electronic degrees of freedom with those of the three-body system, are neglected. Hamiltonian $\hat{H}_{3\mathrm{b}}$ corresponds to the three-body system [37], whereas $\hat{H}_{\mathrm{He}} = -1/2 \sum_j \nabla_j^2 - 2 \sum_j r_j^{-1}$ corresponds to a helium atom with the three-body system considered as the pointlike nucleus with the total charge $Z_f = 2$.

1. Wave functions

Zero-order wave functions of the initial and the final state of the five-particle system corresponding to process (4) are

$$\Psi_{i,f}(\mathbf{R}, \mathbf{r}, \mathbf{r}_1, \mathbf{r}_2) = \phi_{i,f}^{3\mathrm{b}}(\mathbf{R}, \mathbf{r})\phi_{i,f}^e(\mathbf{r}_1, \mathbf{r}_2), \qquad (7)$$

where $\phi_{i,f}^{3\mathrm{b}}(R, r)$ are the three-body-system wave functions; $\phi_{i,f}^e(r_1, r_2)$ are spatial parts of wave functions of the two electrons. The three-body-system wave functions calculated in the adiabatic approximation for the $2p\sigma$ molecular term have the form [37], [23]

$$\phi_{i,f}^{3\mathrm{b}}(\mathbf{R}, \mathbf{r}) = \phi_{2p\sigma}^{\mu}(R, \mathbf{r})\phi_{i,f}^{\mathrm{rel}}(\mathbf{R}), \qquad (8)$$

where $\phi_{2p\sigma}^{\mu}(R, \mathbf{r})$ is the two-center Coulomb function of the muon. Functions $\phi_{i,f}^{\mathrm{rel}}(\mathbf{R})$, describing the relative motion of the nuclei (He^{2+} and h) in the initial (scattering) and the final (molecular) state, are solutions of the Schrödinger

radial equation with spherically symmetric potential $V_{2p\sigma}(R)$ [expressed in μ atomic units (μ a.u.); $m_{h\mu} = e = \hbar = 1$, where $m_{h\mu}$ is the reduced mass of the $h\mu$ atom],

$$V_{2p\sigma}(R) = E_{2p\sigma}(R) + \frac{2}{R} + \frac{U_A(R)}{2M}, \quad (9)$$

where M is the reduced mass of the two nuclei (He^{2+} and h); $E_{2p\sigma}(R)$ is the molecular term, i.e., the energy of the muon moving in the field of the two fixed Coulomb centers, corresponding to the $2p\sigma$ state. United-atom and asymptotic limits of the term $E_{2p\sigma}(0) = -9/8\,\mu$ a.u. and $E_{2p\sigma}(\infty) = -0.5\mu$ a.u., correspond to energies of the muonic lithium ($Z = 3$) in the excited $2p_0$ state and muonic hydrogen ($Z = 1$) in the ground state, respectively; $U_A(R)$ is the adiabatic correction. The initial-state wave function $\phi_i^{\text{rel}}(\mathbf{R})$ contains asymptotically (besides the plane wave) an outgoing spherical wave and is normalized to $(2\pi)^3\delta^3(\mathbf{k}'_i - \mathbf{k}_i)$, where k_i is the initial relative momentum. Partial-wave expansion of the function [38] was used with coefficients $\chi_{k_i L}^i(R)$ describing relative radial motion of the nuclei in the $(h\mu)_{1s} + \text{He}^{++}$ system. The final-state wave function $\phi_f^{\text{rel}}(\mathbf{R}) = \chi_J^f(R)Y_{JM_J}(\hat{R})$, where $\chi_J^f(R)$ describes relative radial motion of the nuclei in the molecular state and $Y_{JM_J}(\hat{R})$ is the spherical function depending on spherical angles of the unit vector $\hat{R}$, is normalized to unity. Electron functions $\phi_{i,f}^e(r_1,r_2)$ are expressed in the independent-particle model [39] with Coulomb repulsion between the two electrons neglected (this approximation is also called the "crude independent-particle approximation" in Ref. [40]). Each of these functions is a symmetrized and antisymmetrized product of single-electron functions for the singlet ($S = 0$) and the triplet ($S = 1$) spin state of the two electrons, respectively. The singly excited state of helium, $\phi_i^e(\mathbf{r}_1,\mathbf{r}_2)$ involves a wave function of one electron in the ground state and the second electron in an excited state. Each function is of the form $u_{n_i l_i}^i(r)Y_{l_i m_i}(\hat{\mathbf{r}})$. For the ground state of helium, 1^1S, the radial function $u_{10}^i(r)$ is taken as a hydrogenlike function $R_{10}(Z_{\text{var}}^{\text{He}}; r)$ with the variational parameter $Z_{\text{var}}^{\text{He}} = 27/16$ [39]. However, another form of the radial function, i.e., the analytical fit to the Hartree-Fock function presented in Ref. [40], is also used in the calculation. For singly excited states $2^{1,3}S$ and $2^{1,3}P$, radial functions $u_{10}^i(r)$ and $u_{2l_i}^i(r)$ are taken from [40]. For singly excited states with $n_i \geqslant 3$, the radial functions are taken as hydrogenlike functions $R_{10}(Z_2^{\text{He}}; r)$ and $R_{n_i l_i}(Z_1^{\text{He}}; r)$ for $Z_2^{\text{He}} = 2$ and $Z_1^{\text{He}} = 1$ (this choice corresponds to the zero-order wave function of Heisenberg's method [39]). The final-state wave function $\phi_f^e(\mathbf{r}_1,\mathbf{r}_2)$ describes one electron bound in the final complex $[(\text{He}\mu h)_J^{2+}, e(n_f l_f m_f)]^+$ and the second freed due to the transition. The corresponding wave functions were chosen in the form of hydrogenlike functions of the discrete, $R_{n_f l_f}(Z_f; r)Y_{l_f m_f}(\mathbf{r})$, and the continuous spectrum,[1] $u_\mathbf{k}(Z_k; \mathbf{r})$, where $\mathbf{k}$ is the momentum of the outgoing Auger electron. The latter function is normalized to $(2\pi)^3\delta(\mathbf{k}' - \mathbf{k})$ and contains asymptotically (besides the plane wave) an incoming spherical wave [38]. Parameters $Z_f = 2$ and $Z_k = 1$

———————

[1] Such functions were exploited in early papers on photoionization of helium [41].

represent the total charge of the muonic molecule and the final complex, respectively.

2. Cross section

The cross section for processes (2) and (3) is given by the Fermi golden rule [38], with the transition amplitude T_{fi} calculated in the first order of perturbation theory for potential (5) and wave functions (7),

$$T_{fi} = \langle \Psi_f | V_{\text{dip}} | \Psi_i \rangle = -\mathbf{d}_{fi} \cdot \mathcal{E}_{fi}, \quad (10)$$

with the molecular and electronic amplitude

$$\mathbf{d}_{fi} = \langle \phi_f^{3b} | \mathbf{d} | \phi_i^{3b} \rangle, \quad (11)$$

and

$$\text{E}_{fi} = \langle \phi_f^e | \text{E} | \phi_i^e \rangle, \quad (12)$$

respectively. By putting wave functions (8) into Eq. (11), one obtains

$$\mathbf{d}_{fi} = -\frac{4\pi}{k_i} \sum_L i^L e^{i\delta_L} d_{JL}(k_i) \sum_{M_L=-L}^{L} Y_{LM_L}^*(\hat{\mathbf{k}}_i)$$
$$\times \sum_{m=-1}^{1} \alpha_m(JM_J; LM_L)\hat{\mathbf{e}}_m^*, \quad (13)$$

where

$$d_{JL}(k_i) = a_1 I_{JL}^{(1)}(k_i) + a_2 I_{JL}^{(2)}(k_i); \quad (14)$$

$a_1 = 1/2 - (m_{\text{He}} - m_{\text{h}})/m_{\text{tot}}$, $a_2 = 1 + 2m_\mu/m_{\text{tot}}$; m_{tot} is the total mass of the molecule; m_c ($c = \text{He}^{2+}, h, \mu$) is the mass of a given component of the molecule; * denotes complex conjugation. The coefficients

$$I_{JL}^{(1)}(k_i) = \int_0^\infty \chi_J^f(R)R\chi_{k_i L}^i(R)\,dR,$$
$$\quad (15)$$
$$I_{JL}^{(2)}(k_i) = \int_0^\infty \chi_J^f(R)\langle\varphi_{2p\sigma}^\mu|\hat{\mathbf{R}}\cdot\mathbf{r}|\varphi_{2p\sigma}^\mu\rangle\chi_{k_i L}^i(R)\,dR$$

are calculated numerically; $\alpha_m(JM_J; LM_L) = -i\sqrt{4\pi/3}\langle Y_{JM_J}|Y_{1m}|Y_{LM_L}\rangle$, and $\hat{\mathbf{e}}_m$ are spherical vectors [42] satisfying the orthogonality relation $\hat{\mathbf{e}}_m^* \cdot \hat{\mathbf{e}}_{m'} = \delta_{mm'}$ for $m, m' = -1,0,1$.

The calculation of the electronic amplitude (12) requires more effort due to the complicated form of wave functions of electrons involved. After tedious calculations exploiting partial expansion of the wave function of the outgoing electron, $u_k(Z_k; \mathbf{r})$, Eq. (12) receives the final form

$$\mathcal{E}_{fi} = 8\pi \sum_{lm} (-i)^l e^{i\delta_l^C} Y_{lm}(\hat{\mathbf{k}}) \sum_{m'=-1}^{1} \mathcal{E}_{n_f l_f m_f; lmm'}^{n_i l_i m_i}(k)\hat{\mathbf{e}}_{m'}, \quad (16)$$

where

$$\mathcal{E}_{n_f l_f m_f; lmm'}^{n_i l_i m_i}(k) = \frac{N_i}{\sqrt{2}}\Big\{ p_{kl_i; n_f l_f}^{n_i l_i} \alpha_{m'}^*(00; l_f m_f)\,\delta_{ll_i}\delta_{mm_i}$$
$$+ q_{n_f 0; kl}^{n_i l_i} \alpha_{m'}^*(l_i m_i; lm)\,\delta_{l_f 0}\delta_{m_f 0}$$
$$+ (-1)^S \big[p_{n_f l_f; kl}^{n_i l_i} \alpha_{m'}^*(00; lm)\,\delta_{l_f l_i}\delta_{m_f m_i}$$
$$+ q_{k0; n_f l_f}^{n_i l_i} \alpha_{m'}^*(m_i l_i; l_f m_f)\,\delta_{l0}\delta_{m0}\big]\Big\}, \quad (17)$$

and

$$p_{n_{\rm f}l_{\rm f};kl}^{n_il_i} = \langle R_{n_{\rm f}l_{\rm f}} | u_{n_il_i}^i \rangle \langle R_{kl} | r^{-2} | u_{10}^i \rangle,$$
$$p_{kl;n_{\rm f}l_{\rm f}}^{n_il_i} = \langle R_{kl} | u_{n_il_i}^i \rangle \langle R_{n_{\rm f}l_{\rm f}} | r^{-2} | u_{10}^i \rangle,$$
$$q_{n_{\rm f}l_{\rm f};kl}^{n_il_i} = \langle R_{n_{\rm f}l_{\rm f}} | u_{10}^i \rangle \langle R_{kl} | r^{-2} | u_{n_il_i}^i \rangle,$$
$$q_{kl;n_{\rm f}l_{\rm f}}^{n_il_i} = \langle R_{kl} | u_{10}^i \rangle \langle R_{n_{\rm f}l_{\rm f}} | r^{-2} | u_{n_il_i}^i \rangle. \tag{18}$$

Each matrix element in (18) denotes radial integral $\int_0^\infty dr\, r^2 \ldots$. The following identities are obvious:

$$p_{n_{\rm f}l_{\rm f};kl}^{10} = q_{n_{\rm f}l_{\rm f};kl}^{10} \quad \text{and} \quad p_{kl;n_{\rm f}l_{\rm f}}^{10} = q_{kl;n_{\rm f}l_{\rm f}}^{10}.$$

After substituting Eqs. (13) and (16) into Eq. (10), one obtains

$$T_{\rm fi} = \frac{2^5 \pi^2}{k_i} \sum_{LM_L} i^L e^{i\delta_L} d_{JL}(k_i) Y_{LM_L}^*(\hat{\mathbf{k}}_i) \sum_{lm} (-i)^l e^{i\delta_l^C} Y_{lm}(\hat{\mathbf{k}})$$
$$\times \sum_{m'=-1}^{1} \mathcal{E}_{n_{\rm f}l_{\rm f}m_{\rm f};lmm'}^{n_il_im_i}(k) \alpha_\mu(JM_J; LM_L), \tag{19}$$

where the value of the momentum of the outgoing electron is determined by energy conservation, $k = 2(\varepsilon_J^{\rm b} - I_{0(1)}^{\rm He} + k_i^2/2M)^{1/2}$, with $I_{0(1)}^{\rm He}$ being the ionization potential of a helium atom (ion).

The cross section corresponding to the transition amplitude (19) then receives the form

$$\sigma = \frac{2^6 \pi}{3} \frac{M}{k_i^3} Q_J^{\rm mol}(k_i) Q_{n_i}^{\rm e}(k), \tag{20}$$

where molecular factor

$$Q_J^{\rm mol}(k_i) = (2J+1) \sum_L (2L+1) \begin{pmatrix} J & L & 1 \\ 0 & 0 & 0 \end{pmatrix}^2 d_{JL}^2(k_i) \tag{21}$$

reduces to a simple expression for $J = 0, 1$, and 2:

$$Q_0^{\rm mol}(k_i) = d_{01}^2(k_i), \tag{22a}$$
$$Q_1^{\rm mol}(k_i) = d_{10}^2(k_i) + 2d_{12}^2(k_i), \tag{22b}$$
$$Q_2^{\rm mol}(k_i) = 2d_{21}^2(k_i) + 3d_{23}^2(k_i). \tag{22c}$$

The electronic factor $Q_{n_i}^e(k)$, averaged over rotational and spin states of the excited helium atom and summed over all energetically allowed electron states of the final complex, takes the form

$$Q_{n_i}^e(k) = \frac{1}{(4-3\delta_{n_i1}) n_i^2} \sum_{n_{\rm f}l_{\rm f}l_i S} (2S+1) Q_{n_{\rm f}l_{\rm f}n_il_iS}^e(k), \tag{23}$$

where partial electronic factor $Q_{n_{\rm f}l_{\rm f}n_il_iS}^e(k)$ is

$$Q_{n_{\rm f}l_{\rm f}n_il_iS}^e(k) = k \sum_{m_im_{\rm f}} \sum_{lm} \sum_{\mu=-1}^{1} \left| \mathcal{E}_{n_{\rm f}l_{\rm f}m_{\rm f};lm\mu}^{n_il_im_i}(k) \right|^2 = N_i^2 \frac{k}{2} \left[\frac{1}{3}(2l_i+1)(2l_{\rm f}+1) \begin{pmatrix} l_i & l_{\rm f} & 1 \\ 0 & 0 & 0 \end{pmatrix}^2 \left(q_{k0;n_{\rm f}l_{\rm f}}^{n_il_i} \right)^2 \right.$$
$$+ (2l_i+1)\left(p_{n_{\rm f}l_{\rm f};k1}^{n_il_i} \right)^2 \delta_{l_il_{\rm f}} + (2l_i+1)\left(p_{kl;n_{\rm f}}^{n_il_i} \right)^2 \delta_{l_{\rm f}1} + l_i \left(q_{n_{\rm f}0;k|l_i-1|}^{n_il_i} \right)^2 \delta_{l_{\rm f}0} + (l_i+1)\left(q_{n_{\rm f}0;kl_i+1}^{n_il_i} \right)^2 \delta_{l_{\rm f}0}$$
$$+ (-1)^S 2 \left(p_{k1;n_{\rm f}1}^{n_i1} p_{n_{\rm f}1;k1}^{n_i1} \delta_{l_i1}\delta_{l_{\rm f}1} + p_{k0;n_{\rm f}1}^{n_i0} q_{k0;n_{\rm f}1}^{n_i0} \delta_{l_i0}\delta_{l_{\rm f}1} + q_{k0;n_{\rm f}0}^{n_i1} q_{n_{\rm f}0;k0}^{n_i1} \delta_{l_i1}\delta_{l_{\rm f}0} + p_{n_{\rm f}0;k1}^{n_i0} q_{n_{\rm f}0;k1}^{n_i0} \delta_{l_i0}\delta_{l_{\rm f}0} \right) \right]. \tag{24}$$

For the formation process with a helium atom in the ground state, the electronic factor reduces to the simple expression

$$Q_1^e(k) = (k/2) \sum_{n_{\rm f}=1}^{n_{\rm f,max}} \left(p_{n_{\rm f}0;k1}^{10} \right)^2$$
$$+ (5k/12) \sum_{n_{\rm f}=2}^{n_{\rm f,max}} \left(p_{k0;n_{\rm f}1}^{10} \right)^2. \tag{25}$$

In all previous calculations ([20,29,30,33]), hydrogenlike functions $R_{10}(Z_{\rm var}^{\rm He}; r)$ describing ground-state electrons were used, as well as the following condition:

$$Z_{\rm f} = Z_{\rm k} = Z_{\rm var}^{\rm He} = 27/16, \tag{26}$$

which eliminates from Eq. (25) the contribution of electron excited states of the final complex. Consequently, the electronic factor (25) reduces to a simple expression,

$$Q_1^e(k) = k \left(p_{10;k1}^{10} \right)^2 / 2. \tag{27}$$

The cross section for the formation of the muonic molecule due to collision with a helium ion,

$$(h\mu)_{1s} + [\text{He}^{2+}, e(n_il_im_i)]^+ \rightarrow (\text{He}\mu h)_J^{2+} + e, \tag{28}$$
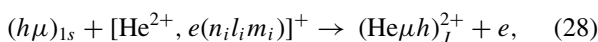
is given by Eq. (20) with the molecular factor (22) and the electronic factor (averaged over rotational and spin states of the excited helium ion)

$$Q_{n_i}^e(k) = \frac{k}{4n_i^2} \sum_{l_il} (2l+1)(2l_i+1) \begin{pmatrix} l & l_i & 1 \\ 0 & 0 & 0 \end{pmatrix}^2$$
$$\times \left| \langle R_{kl} | r^{-2} | R_{n_il_i} \rangle \right|^2. \tag{29}$$

Reaction rates normalized to LHD and corresponding to formation processes (2) and (3) are calculated as $\lambda = N_0 v\sigma$.

B. Auger formation in triple H-H′-He gas mixtures

Collision energies corresponding to resonances presented in Table I are practically unattainable in binary hydrogen-helium gas mixtures at room temperature. Although the initial kinetic energies of $d\mu$ and $t\mu$ atoms, i.e., just after reaching their ground states, are very poorly known, some Monte Carlo simulations indicate the presence of fractions of fast (nonthermalized) muonic atoms in the ground states: $d\mu$ in D_2 [43] and $t\mu$ in the D-T mixture [44]. Experimentally estimated initial energies of the fast atoms are on the level

of several eV [45], i.e., well below the resonant energies presented in Table I. However, the ground-state muon transfer from a lighter to heavier hydrogen isotope leads to a significant acceleration of the resulting muonic atoms (kinetic energies are given in parentheses),

$$p\mu + d \rightarrow d\mu \ (43.2 \text{ eV}) + p \ (91.2 \text{ eV}),$$
$$p\mu + t \rightarrow t\mu \ (44.5 \text{ eV}) + p \ (138.2 \text{ eV}), \quad (30)$$
$$d\mu + t \rightarrow t\mu \ (18.9 \text{ eV}) + d \ (29.4 \text{ eV}).$$

These processes occur in triple H-H′-He gas mixtures, where H and H′ represent two different hydrogen isotopes. It can, therefore, be expected that the resonantly enhanced formation of $(^{3,4}\text{He}\mu d)_2^{2+}$ and $(^{3,4}\text{He}\mu t)_2^{2+}$ molecules will occur in H-D-He, H-T-He, and D-T-He mixtures even at room temperature. However, possible deceleration of the atoms due to collisions with surrounding hydrogen isotope molecules and helium atoms may reduce the effect. On the other hand, results presented in Refs. [46] show that the deceleration rate of $d\mu$ in D_2 as well as $t\mu$ in D-T and H-D-T mixtures from energies of several tens of eV to about 1 eV is of the order of 10^9s^{-1}, which is comparable to the resonant values of the formation rates for the above muonic molecules. Furthermore, cross sections for $d\mu + H_2$ and $t\mu + H_2$ scattering is significantly suppressed by the strong Ramsauer-Townsend effect in the collision energy range 2–30 eV [36,47]. This fact suggests that in the triple H-D-He and H-T-He gas mixtures containing a dominating admixture of H_2 molecules, the thermalization will be significantly weaker, which may allow the resonant formation.

Formation rates corresponding to a triple H-H′-He gas mixture in thermal equilibrium can be obtained by averaging the corresponding bare rates over the collision energy distribution,

$$\lambda(T, E_{h\mu}) = \int_0^\infty \lambda(\varepsilon) f(\varepsilon; E_{h\mu}, T) d\varepsilon, \quad (31)$$

where

$$f(\varepsilon; E_{h\mu}, T) = \sqrt{\frac{m_{h\mu} \ m_{\text{He}}}{4\pi T E_{h\mu}}} \frac{1}{m_r} \{\exp[-m_{\text{He}}(v - v_{h\mu})^2/(2T)]$$
$$- \exp[-m_{\text{He}}(v + v_{h\mu})^2/(2T)]\}; \quad (32)$$

ε and $E_{h\mu}$ are the collision energy and the kinetic energy of the $h\mu$ atom in the laboratory frame, respectively; $v = \sqrt{2\varepsilon/m_r}$ and $v_{h\mu} = \sqrt{2E_{h\mu}/m_{h\mu}}$ are the corresponding velocities; T is the temperature of the triple mixture expressed in eV; $\lambda(\varepsilon)$ is the bare formation rate calculated in Sec. II A2 as a function of collision energy; $m_{h\mu}$, m_{He}, and m_r are the mass of muonic hydrogen isotope atom, the mass of helium atom, and the reduced mass of the two atoms, respectively. Equation (32) was derived using the idea of [48], i.e., from the joint velocity distribution $f(\boldsymbol{v}_{\text{He}}, \boldsymbol{v}_{h\mu} - \boldsymbol{v}'_{h\mu})$ being a product of the Maxwell distribution corresponding to helium atoms and Dirac delta function $\delta^3(\boldsymbol{v}_{h\mu} - \boldsymbol{v}'_{h\mu})$ corresponding to muonic atoms, where $\boldsymbol{v}_{\text{He}}$ is the velocity of the He atom. After the change of variables $(\boldsymbol{v}_{\text{He}}, \boldsymbol{v}'_{h\mu}) \rightarrow (\boldsymbol{v}_{\text{CM}}, \boldsymbol{v})$, where $\boldsymbol{v}_{\text{CM}}$ is the velocity of center of

mass of the $h\mu + \text{He}$ system, and integration over $d^3 v_{\text{CM}}$ and directions of $\boldsymbol{v}$, one obtains Eq. (32).

C. Auger formation in H-He plasma

It can be expected that the resonant enhancement of the Auger formation of muonic molecules can also occur in hydrogen-helium plasma at temperatures greater than 1 eV, provided that the plasma contains significant amounts of helium atoms and ions (He^+). According to theoretical considerations presented in Ref. [49], the plasma is almost completely ionized at a temperature comparable to ionization energy of a helium ion (54.4 eV). Thus, the plasma temperature should satisfy the condition $1 \text{ eV} \leqslant T \leqslant 50 \text{ eV}$ (or $10^4 \text{ K} \leqslant T \leqslant 6 \times 10^5 \text{ K}$).

Atomic and molecular processes induced by muons in D-T plasma have been studied theoretically in Ref. [50]. In particular, the authors suggest that formation of the $dt\mu$ molecule due to three-particle collisions in dense plasma with density $\phi \sim 1 \text{ LHD}$ dominates, as the corresponding formation rate is proportional to ϕ^2. However, if D_2 or DT molecules are present in the plasma, then the resonant formation of weakly bound state $(J, \upsilon) = (1, 1)$ of the $dt\mu$ molecule due to Vesman's mechanism must also be taken into account. At the same time, the authors neglect formation due to the Auger process, which is much slower for lower-lying states and energetically forbidden for the weakly bound state. After the formation, collision-induced breakup of the molecule will take place if collision energy exceeds the binding energy threshold. So, the breakup becomes important if the plasma temperature increases. As for H-He plasma, it is very likely that the formation of $(\text{He}\mu h)_J^{2+}$ molecules due to analogous three-particle collisions will also dominate for dense plasma. However, for densities not exceeding 0.1 LHD, one can expect that the molecules will be formed mainly due to Auger processes, as the three-particle collisions will be suppressed. At the same time, collision-induced breakup restoring the $(h\mu)_{1s} + \text{He}^{2+}$ system in the $2p\sigma$ state (which is a threshold process), as well as the spontaneous and collision-induced deexcitation to the unbound $1s\sigma$ state, will also take place.

In this section, the calculation of average reaction rates corresponding to Auger formation in H-He plasma in thermal equilibrium at temperature $T \leqslant 50 \text{ eV}$ is presented for three plasma densities, namely, $\phi = 10^{-5}$, 10^{-3}, and 0.1 LHD.

The electrostatic interaction of components of H-He plasma leads to a broadening and shifts of energy levels of hydrogen and helium atoms and ions, as well as to lowering of the corresponding ionization potentials (the so-called depression of the continuum). In the present approximate calculation, the treatment analogous to the one presented in Ref. [51] is exploited, i.e., unperturbed energy levels of the atoms and ions present in H-He plasma are used, whereas the depression of the continuum is taken into account using the Debye-Hueckel theory [49]. Populations of excited states of helium atoms and ions depend on plasma temperature and number density of free electrons. The latter can be obtained using the standard procedure described in Refs. [52]. It is based on solving the system of coupled equations, which depend on the fraction of free electrons x_e, fraction of hydrogen atoms x_0^H, helium atoms

x_0^{He}, and fractions of their corresponding ions: x_1^{H}, x_1^{He}, x_2^{He},

$$x_0^{\mathrm{H}} + x_1^{\mathrm{H}} + c_{\mathrm{He}} = 1, \quad x_1^{\mathrm{H}}/x_0^{\mathrm{H}} = f_0^{\mathrm{H}}(T),$$
$$x_0^{\mathrm{He}} + x_1^{\mathrm{He}} + x_2^{\mathrm{He}} = c_{\mathrm{He}}, \quad x_1^{\mathrm{He}}/x_0^{\mathrm{He}} = f_0^{\mathrm{He}}(T),$$
$$x_e = x_1^{\mathrm{H}} + x_1^{\mathrm{He}} + 2x_2^{\mathrm{He}}, \quad x_2^{\mathrm{He}}/x_1^{\mathrm{He}} = f_1^{\mathrm{He}}(T),$$
$$(33)$$

where $x_e = N_e/N_{\mathrm{tot}}$ and $x_r^{\mathrm{A}} = N_r^{\mathrm{A}}/N_{\mathrm{tot}}$; N_e and N_r^{A} denotes the number density of free electrons and r ion of type A = H, He, respectively ($r = 0$ for H and He, $r = 1$ for H$^+$ and He$^+$, and $r = 2$ for He^{2+}); $N_{\mathrm{tot}} = \sum_{\mathrm{A},r} N_r^{\mathrm{A}}$ is the number density of the plasma, also referred to as plasma density (the sum does not include N_e in the present treatment); $c_{\mathrm{He}} = \sum_{r=0}^{2} N_r^{\mathrm{He}}/N_{\mathrm{tot}}$ is the relative concentration of helium. Functions $f_r^{\mathrm{A}}(T)$ are determined by Saha formula [51–53]

$$f_r^{\mathrm{A}}(T) = \frac{G_{r+1}^{\mathrm{A}}(T)}{G_r^{\mathrm{A}}(T)} \left(m_{r+1}^{\mathrm{A}}/m_r^{\mathrm{A}}\right)^{3/2} e^{-\eta_e} \exp\left(-\tilde{I}_r^{\mathrm{A}}/T\right), \quad (34)$$

where $\tilde{I}_r^{\mathrm{A}} = I_r^{\mathrm{A}} - \Delta I_r^{\mathrm{A}}$ is the transition energy between ground states of r- and $(r + 1)$ ion of type A (the ionization potential of r ion), I_r^{A}, reduced by depression of the continuum ΔI_r^{A}; η_e is the degeneracy parameter of electron gas [49]; m_r^{A} is the mass of r ion of type A; however, the difference between m_{r+1}^{A} and m_r^{A} is neglected in the present calculation, i.e., $m_{r+1}^{\mathrm{A}}/m_r^{\mathrm{A}} = 1$; $G_r^{\mathrm{A}}(T) = \sum_{n=1}^{n_r^{\mathrm{A}}} g_{r,n}^{\mathrm{A}} \exp(-\varepsilon_{r,n}^{\mathrm{A}}/T)$ is the partition function containing summation over energy levels of bound states,[2] and $g_{r,n}^{\mathrm{A}}$ and $\varepsilon_{r,n}^{\mathrm{A}}$ are the corresponding statistical weights and excitation energies (calculated relative to the ground-state energy), respectively. The excitation energy of an excited atom and ion is approximated by the formula $\varepsilon_{r,n}^{\mathrm{A}} = I_r^{\mathrm{A}} - 2^{-1}(Z_{r+1}^{\mathrm{A}}/n)^2$, where $r = 0,1$ and $Z_r^{\mathrm{A}} = r$. For a completely ionized hydrogen and helium atom, one has $G_1^{\mathrm{H}}(T) = G_2^{\mathrm{He}}(T) = 1$ [54]. It is a known fact that populations of excited states of atoms and ions present in low-temperature plasma are significantly smaller than populations of their ground-state counterparts as well as bare nuclei [49]. One can expect, therefore, that an excited helium atom or ion present in H-He plasma is surrounded by the ground-state hydrogen and helium atoms and ions (He$^+$), as well as by H$^+$ and He^{++} nuclei. Using this fact, one can estimate the maximal principal quantum number n_r^{A} appearing in the partition function $G_r^{\mathrm{A}}(T)$ using the simple relation $a_{r,n}^{\mathrm{A}} + a_{r',1}^{\mathrm{A}'} \leqslant d$, where $a_{r,n}^{\mathrm{A}} = n^2/Z_{r+1}^{\mathrm{A}}$ is the Bohr radius of an excited electron orbit of hydrogen and helium atom or ion (for complete ionization, one has $a_{1,n}^{\mathrm{H}} = 0$ and $a_{2,n}^{\mathrm{He}} = 0$); $d = N_{\mathrm{tot}}^{-1/3}$ is an estimate of the average distance between any two neighboring nuclei present in the plasma. The density of the plasma considered here does not exceed 0.1 LHD (6.29×10^{-4} in atomic units). Consequently, $d \geqslant 11.7 \gg 1$ and, neglecting $a_{r',1}^{\mathrm{A}'} \propto 1$, one obtains $n \leqslant \sqrt{Z_{r+1}^{\mathrm{A}} d}$. Another upper bound for n comes from the depression of the continuum [51], i.e., $\varepsilon_{r,n}^{\mathrm{A}} \leqslant \tilde{I}_r^{\mathrm{A}}$, and results in $n \leqslant Z_{r+1}^{\mathrm{A}}/\sqrt{2\Delta I_r^{\mathrm{A}}}$. The final restriction for n is then $n \leqslant n_r^{\mathrm{A}} = \min(\sqrt{Z_{r+1}^{\mathrm{A}} d}, Z_{r+1}^{\mathrm{A}}/\sqrt{2\Delta I_r^{\mathrm{A}}})$. At the

---

[2]Subscript "i" of the principal quantum number of helium atom and ion is now omitted to simplify the notation.

same time, factor $e^{-\eta_e}$ involved in Eq. (34) can be replaced with a high accuracy by $g_e(T/2\pi)^{3/2}/N_e$, where $g_e = 2$ is the statistical weight of the electron [54]. After simple calculation, one obtains from (33) a single equation for x_e,

$$x_e = (1 - c_{\mathrm{He}})\frac{f_0^{\mathrm{H}}(T)}{1 + f_0^{\mathrm{H}}(T)} + c_{\mathrm{He}}\frac{f_0^{\mathrm{He}}(T)\left[1 + 2f_1^{\mathrm{He}}(T)\right]}{1 + f_0^{\mathrm{He}}(T)\left[1 + f_1^{\mathrm{He}}(T)\right]},$$
$$(35)$$

which can be solved numerically only as $f_r^{\mathrm{A}}(T)$ depends on x_e. Depression of the continuum expressed in the Debye-Hueckel theory equals $\Delta I_r^{\mathrm{A}} = Z_{r+1}^{\mathrm{A}}/\lambda_D$, where $\lambda_D = \sqrt{T/\{4\pi[N_e + \sum_{\mathrm{A},r}(Z_r^{\mathrm{A}})^2 N_r^{\mathrm{A}}]\}}$ is the Debye shielding radius, which can be expressed in the following form: $\lambda_D = \sqrt{T/[8\pi N_{\mathrm{tot}}(x_e + x_2^{\mathrm{He}})]}$, where, from Eqs. (33), $x_2^{\mathrm{He}} = c_{\mathrm{He}} f_0^{\mathrm{He}}(T)f_1^{\mathrm{He}}(T)/\{1 + f_0^{\mathrm{He}}(T)[1 + f_1^{\mathrm{He}}(T)]\}$. The low-temperature limit of x_e obtained from (35) is $x_e \approx f_0^{\mathrm{H}}(T)(1 - c_{\mathrm{He}})$ and tends to zero for $T \to 0$, whereas the high-temperature limit of x_e is simply $x_e = 1 + c_{\mathrm{He}}$, as all hydrogen and helium atoms are fully ionized for $T \to \infty$. The Debye-Hueckel theory is justified when $\lambda_D \geqslant [8\pi N_{\mathrm{tot}}(1 + x_e)]^{-1/3}$ [51]. It was proved by numerical calculation that this inequality is fulfilled for the following considered plasma conditions: 1 eV $\leqslant T \leqslant$ 50 eV, 10^{-5} LHD $\leqslant N_{\mathrm{tot}} \leqslant 0.1$ LHD, and $0.1 \leqslant c_{\mathrm{He}} \leqslant 0.9$. The population $P_{r,n}$ of excited helium atoms and ions in the ground ($n = 1$) and excited ($n \geqslant 2$) state calculated relative to the total number density of helium ($N_{\mathrm{tot}}^{\mathrm{He}} = \sum_{r,n} N_{r,n}^{\mathrm{He}}$) is

$$P_{r,n} = \frac{N_{r,n}^{\mathrm{He}}}{N_{\mathrm{tot}}^{\mathrm{He}}} = \left(\sum_{q=0}^{2}\sum_{m=1}^{n_q^{\mathrm{He}}} \frac{N_{q,m}^{\mathrm{He}}}{N_{r,n}^{\mathrm{He}}}\right)^{-1}, \quad (36)$$

where $N_{r,n}^{\mathrm{He}}$ is the number density of excited helium atoms or ions. For $r = 2$, it is assumed that $n_2^{\mathrm{He}} = 1$ and the corresponding population $P_{2,1}$ and number density $N_{2,1}^{\mathrm{He}}$ of He^{2+} ions is denoted by P_2 and N_2^{He}, respectively. According to Refs. [53], the ratio $N_{q,m}^{\mathrm{He}}/N_{r,n}^{\mathrm{He}}$ is determined for $q = r$ by the Boltzmann distribution,

$$\frac{N_{r,m}^{\mathrm{He}}}{N_{r,n}^{\mathrm{He}}} = \frac{g_{r,m}^{\mathrm{He}}}{g_{r,n}^{\mathrm{He}}} \exp\left[(\varepsilon_{r,n}^{\mathrm{He}} - \varepsilon_{r,m}^{\mathrm{He}})/T\right], \quad (37)$$

whereas, for $q = r + 1$, the ratio is determined by the Saha formula,

$$\frac{N_{r+1,m}^{\mathrm{He}}}{N_{r,n}^{\mathrm{He}}} = \frac{g_e}{N_e}\frac{g_{r+1,m}^{\mathrm{He}}}{g_{r,n}^{\mathrm{He}}}\left(\frac{T}{2\pi}\right)^{3/2}$$
$$\times \exp\left[-\left(\tilde{I}_r^{\mathrm{He}} + \varepsilon_{r+1,m}^{\mathrm{He}} - \varepsilon_{r,n}^{\mathrm{He}}\right)/T\right]. \quad (38)$$

The population of fully ionized helium atoms, P_2, can be expressed as $P_2 = 1 - \sum_{r=0}^{1}\sum_{n=1}^{n_r^{\mathrm{He}}} P_{r,n}$.

The effective formation rate, which can be measured experimentally in H-He plasma, is $\lambda = c_{\mathrm{He}}\phi\lambda_{\mathrm{av}}$, where λ_{av} is the average rate obtained from the corresponding bare rates $\lambda_{r,n}(\varepsilon)$ [$r = 0$ for process (2) and $r = 1$ for process (3)]

by averaging the latter over the Maxwell distribution of the collision energy and populations $P_{r,n}$,

$$\lambda_{av} = \sum_{r=0}^{1} \sum_{n=1}^{n_r^{He}} P_{r,n} \lambda_{r,n}^{Maxw.}, \tag{39a}$$

where

$$\lambda_{r,n}^{Maxw.} = \int_0^\infty \lambda_{r,n}(\varepsilon) f_{Max}(T,\varepsilon)\, d\varepsilon, \tag{39b}$$

and $f_{Max}(T,\varepsilon) = 2\sqrt{\varepsilon/\pi}\, T^{-3/2} \exp(-\varepsilon/T)$ is the Maxwell distribution.

III. RESULTS AND DISCUSSION

A. Formation rates corresponding to collisions with the ground-state helium atoms

The rates corresponding to cross section (20) for $n_i = 1$ and electronic factor (27) are presented in Fig. 2 for the $(^3\text{He}\mu p)_{0,1}^{2+}$, $(^4\text{He}\mu p)_0^{2+}$, $(^4\text{He}\mu d)_{0,1,2}^{2+}$, and $(^{3,4}\text{He}\mu t)_{0,1,2}^{2+}$ molecules (reaction rates for the formation of $(^3\text{He}\mu d)_{0,1,2}^{2+}$ and $(^4\text{He}\mu p)_1^{2+}$ were presented in Ref. [33]). As is seen from the figure, formation rates for the $(^3\text{He}\mu p)_1^{2+}$, $(^4\text{He}\mu d)_2^{2+}$, $(^3\text{He}\mu t)_2^{2+}$, and $(^4\text{He}\mu t)_2^{2+}$ molecules are significantly enhanced near collision

energies corresponding to shape resonances in $(h\mu)_{1s} + \text{He}^{2+}$ scattering. Maximal values of the rates are of the order of 10^8–10^9 s^{-1}. The resonances influence the formation rates via radial function $\chi_{k_i L}^i(R)$, which calculated for a resonant energy has a large amplitude in the region of $V_{2p\sigma}(R)$ potential well, where the radial function of the bound (molecular) state, $\chi_J^f(R)$, is localized. As a result, integrals (15) and hence coefficients $d_{JL}(k_i)$, given by Eq. (14), and molecular factors (22) receive large values.

The formation rates presented in Fig. 2 for rotational states $J = 0$ are negligibly small at slow collisions, in contrast to the rates for $J = 1$. This is due to the fact that the former states are formed due to the $L = 1 \rightarrow J = 0$ transition and, consequently, radial function $\chi_{k_i 1}^i(R)$ is suppressed by the centrifugal potential barrier in the region where $\chi_0^f(R)$ is localized. As a result, the corresponding coefficient $d_{01}(k_i)$ entering molecular factor (22a) receives small values [the similar situation is in the case of the formation of the $(^4\text{He}\mu t)_2^{2+}$ molecule, which is dominated by a $1 \rightarrow 2$ transition at slow collisions]. At the same time, the formation of the rotational state $J = 1$ is dominated by a $0 \rightarrow 1$ transition at slow collisions and, consequently, radial function $\chi_{k_i 0}^i(R)$, which is not suppressed by a centrifugal barrier, leads to a relatively large value of coefficient $d_{10}(k_i)$, which dominates
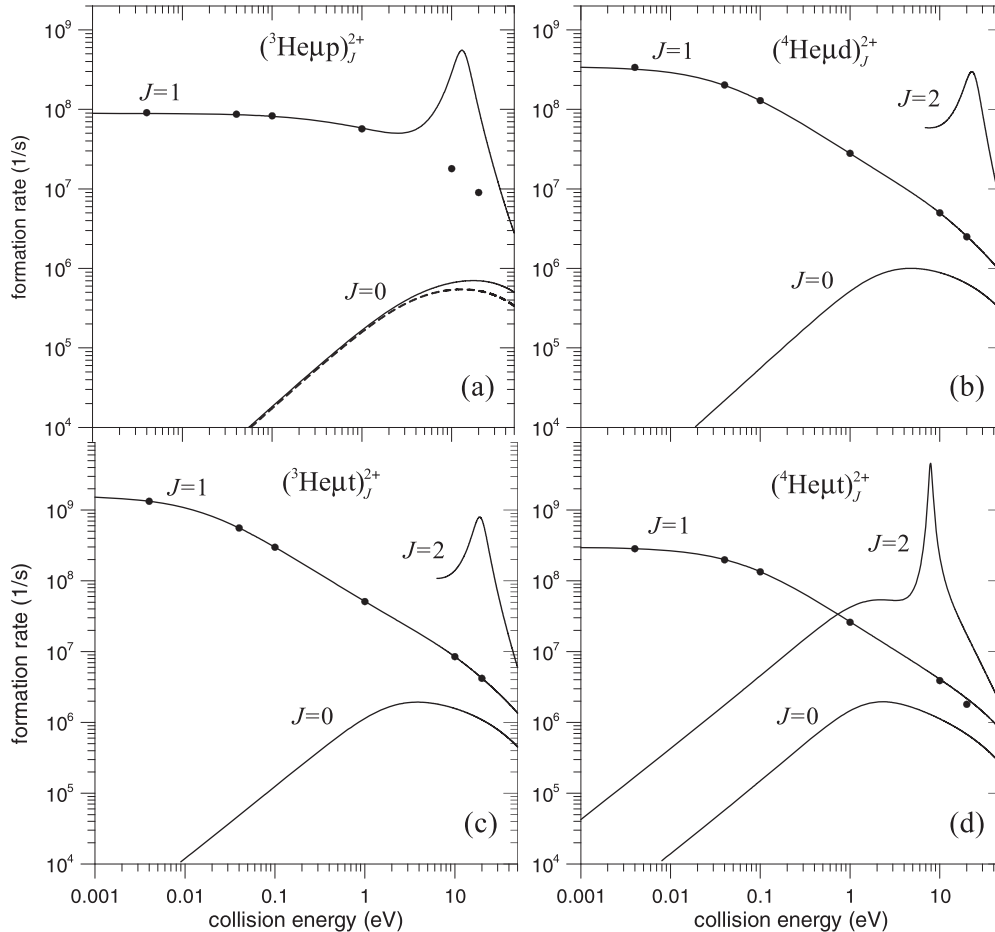
FIG. 2. Formation rates (normalized to LHD) corresponding to the collision of a muonic hydrogen isotope atom with the ground-state helium atom. Black dots represent the results obtained in Ref. [20] for $J = 1$. Dashed line in (a) represents the formation rate for the $(^4\text{He}\mu p)_0^{++}$ molecule.

in molecular factor (22b). Thresholds of 6.9 and 6.4 eV exist for the formation of the $(^4\mathrm{He}\mu d)_2^{++}$ and $(^3\mathrm{He}\mu t)_2^{++}$ molecules since their binding energies, 17.7 and 18.2 eV, are smaller than the ionization potential of the helium atom, $I_0^{\mathrm{He}} = 24.6$ eV.

The dots in Fig. 2 represent the results obtained in Ref. [20] for the rotational state of the molecules $J = 1$. The results coincide with the present ones for the $(^4\mathrm{He}\mu d)_1^{2+}$ and $(^{3,4}\mathrm{He}\mu t)_1^{2+}$ molecules for all collision energies, whereas for $(^3\mathrm{He}\mu p)_1^{2+}$, they coincide at slow collisions and differ by about two and one orders of magnitude at 10 and 20 eV, respectively. The difference is due to the resonance in elastic $(p\mu)_{1s} + {}^3\mathrm{He}^{2+}$ scattering at 12.9 eV for partial wave $L = 2$ (see Table I), whose contribution was omitted in [20]. At the same time, all formation rates for $J = 1$ corresponding to slow collisions are in good agreement (within an order of magnitude) with the rates measured experimentally [32] in low-temperature binary H-He mixtures[3] where s-wave scattering, populating the rotational state $J = 1$, dominates. It is therefore clear why the resonant enhancement of the formation of $(^{3,4}\mathrm{He}\mu p)_1^{2+}$

_____

[3] The exception is the experiment of Gartner *et al.* [32] where a very small admixture of H_2 and HD molecules in D-He targets was added.

molecules corresponding to collision energies above 7 eV has not been found experimentally so far.

Reaction rates for the formation of muonic molecules depend on electron wave functions used in calculation. An independent-particle approximation was used in [20] for the description of the conversion electron. According to the authors, the variation of the total charge Z_k of the final complex, $[(\mathrm{He}\mu h)^{2+}, e(1s)]^+$, between 1 and $Z_{\mathrm{var}}^{\mathrm{He}}$ changes the formation rates by about 20–40%. At the same time, the results of Ref. [29] obtained without inclusion of electron screening and using static approximation for the description of the interaction of the final system with the Auger electron differ from those of [20] by about 6%. According to [29], the inclusion of electron screening in the initial channel of the formation process increases the corresponding rates by up to 70% at energies below 0.02 eV. Above 0.1 eV, the electron screening is practically unimportant. In the present calculation concerning relatively fast collisions ($\varepsilon \geqslant 0.1$ eV), the electron screening is neglected. In order to determine how the results change with variation of the charges involved in the formation process, constraint (26) must be abandoned and the electronic factor (25) should be used. Results obtained show that the electronic factor is much less sensitive to a variation of Z_f than Z_k. Namely, the variation of Z_f from $Z_{\mathrm{var}}^{\mathrm{He}}$

FIG. 3. (Color online) Formation rates (normalized to LHD) corresponding to the collision of a muonic hydrogen isotope with a singly excited helium atom for different principal quantum numbers of excited electron.

to 2 (with the remaining charges equal to $Z_{\text{var}}^{\text{He}}$) reduces the electronic factor (25) (and the resulting formation rates) by less than 5%, whereas variation of Z_k from $Z_{\text{var}}^{\text{He}}$ to 1 (with the remaining charges equal to $Z_{\text{var}}^{\text{He}}$) reduces the electronic factor by at most 50%. The reduction is maximal for slow collisions and small binding energies of the muonic molecules, i.e., for small values of the momentum of the Auger electron. At the same time, the electronic factor (25) calculated using an analytical fit to the Hartree-Fock wave function of the ground-state helium electrons [40], and the charges $Z_f = 2$ and $Z_k = 1$, is about 60% smaller than the electronic factor (27) calculated using the variational function $R_{10}(Z_{\text{var}}^{\text{He}}; r)$ and the condition (26).

B. Formation rates corresponding to collisions with excited helium atoms and ions

Formation rates for process (4) for $n_i \geqslant 2$ are calculated using cross section (20) with the electronic factor defined by Eqs. (23) and (24). Characteristic examples of the formation rates are presented in Fig. 3 for $n_i = 2$–5 and 10. The rates for $n_i = 2$ are several times smaller than their counterparts, corresponding to collisions with the ground-state helium atoms. The results very weakly depend on n_i in the whole

collision energy range considered if the binding energies of the molecules exceed the ionization potential of the helium ion, $\varepsilon_J^b > I_1^{\text{He}} = 2$ (54.4 eV). According to Table I, this holds for molecules in the rotational ground state, $J = 0$, and for molecules $({}^4\text{He}\mu d)_1^{2+}$ and $({}^4\text{He}\mu t)_1^{2+}$. Exemplary results are presented in Figs. 3(a) and 3(b) for $({}^3\text{He}\mu d)_0^{2+}$ and $({}^4\text{He}\mu t)_1^{2+}$, respectively. Formation rates for molecules with $\varepsilon_J^b < I_1^{\text{He}}$ significantly decrease with increasing n_i for collision energies below thresholds $I_1^{\text{He}} - \varepsilon_J^b$, whereas above the thresholds, they reveal a very weak n_i dependence. The corresponding examples are presented in Fig. 3(c) and 3(d) for $({}^4\text{He}\mu p)_1^{2+}$ and $({}^3\text{He}\mu d)_2^{2+}$, respectively. This n_i dependence of the formation rates can be explained in the following way. It was proved by numerical calculation that the dominant contribution to the average electronic factor (23) comes from electron bound states of the final complex, $[(\text{He}\mu h)_J^{2+}, e(n_f l_f m_f)]^+$, with n_f belonging to the interval $\Delta_{n_f} = [n_i, n_i + \delta n_i]$, where δn_i increases from 0 (for $n_i = 2$) to 4 (for $n_i = 10$). These n_f states are called the relevant n_f states hereafter. Numerical results show that $Q_{n_i}^e(k)$ (and, consequently, the formation rate) exhibits weak n_i dependence when all of the relevant n_f states are energetically allowed and included in Eq. (23). At the same time, the ionization energy corresponding to the transition from He* to the final complex can be approximated
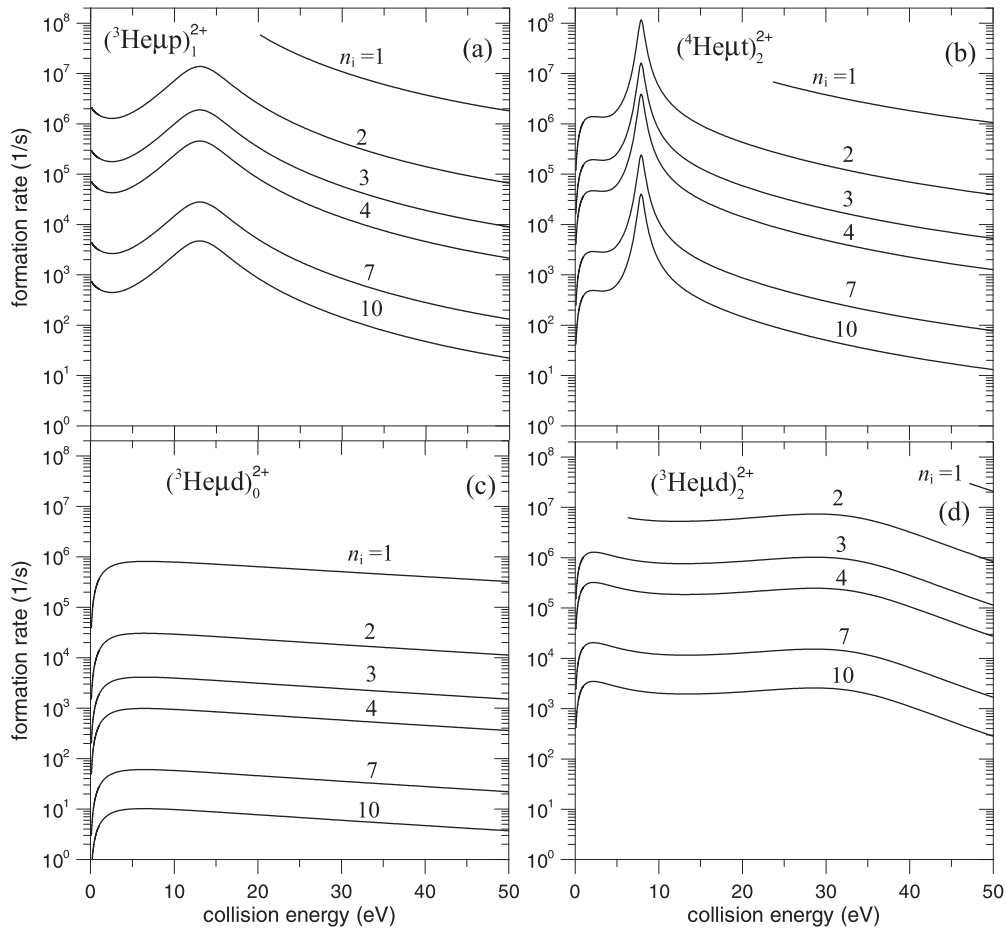
FIG. 4. Formation rates (normalized to LHD) corresponding to the collision of a muonic hydrogen isotope atom with an excited helium ion for different principal quantum numbers.

by the expression $2 + (2n_i^2)^{-1} - 2n_f^{-2}$, which for the relevant n_f states is an increasing function of n_i and tends to the limit $I_1^{\text{He}} = 2$. If binding energies of the molecules fulfill the condition $\varepsilon_J^b > I_1^{\text{He}}$, then all relevant n_f states are energetically allowed (for all collision energies) and included in Eq. (23). If binding energies satisfy the condition $\varepsilon_J^b < I_1^{\text{He}}$, then all of the relevant n_f states are energetically allowed for collision energies exceeding the thresholds $I_1^{\text{He}} - \varepsilon_J^b$. Below the thresholds, some of the states, which are energetically forbidden, are excluded from (23) and, as a consequence, formation rates reveal strong n_i dependence. The rates possess then numerous jumps, corresponding to zero momentum of the Auger electron and resulting from electron excitations of the final complex.

The formation rates corresponding to collisions with helium ion (28) are presented in Fig. 4 for the $(^3\text{He}\mu p)_1^{2+}$, $(^4\text{He}\mu t)_2^{2+}$, $(^3\text{He}\mu d)_0^{2+}$, and $(^3\text{He}\mu d)_2^{2+}$ molecules, for the principal quantum number of the ion $n_i = 1-4, 7, 10$. The rates decrease with increasing n_i. Resonant peaks are clearly pronounced in the reaction rates corresponding to (a) $(^3\text{He}\mu p)_1^{2+}$ and (b) $(^4\text{He}\mu t)_2^{2+}$ formed due to collisions with excited helium ions. For collisions with the ground-state ones, energy thresholds situated above the corresponding resonant energies cut off the resonant peaks. The same holds for the (d) $(^3\text{He}\mu d)_2^{2+}$ molecule; however, the resonant enhancement of the
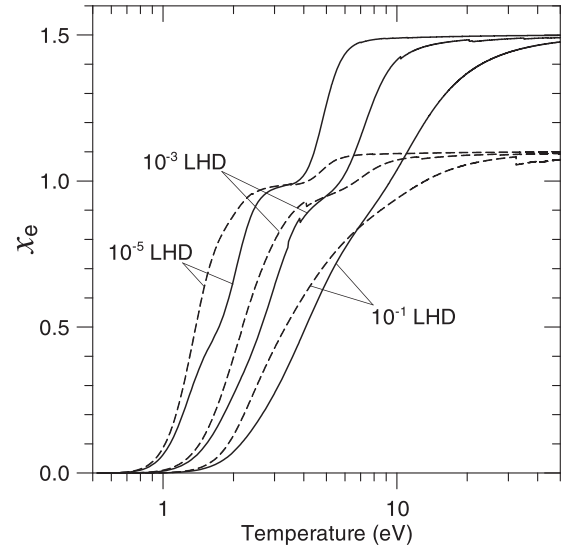
FIG. 6. Fraction of free electrons in H-He plasma as a function of temperature, calculated for helium relative concentrations $c_{\text{He}} = 0.5$ (solid curve) and $c_{\text{He}} = 0.1$ (dashed curve), and three plasma densities indicated on curves.

corresponding formation rate is very weakly pronounced at about 30 eV.
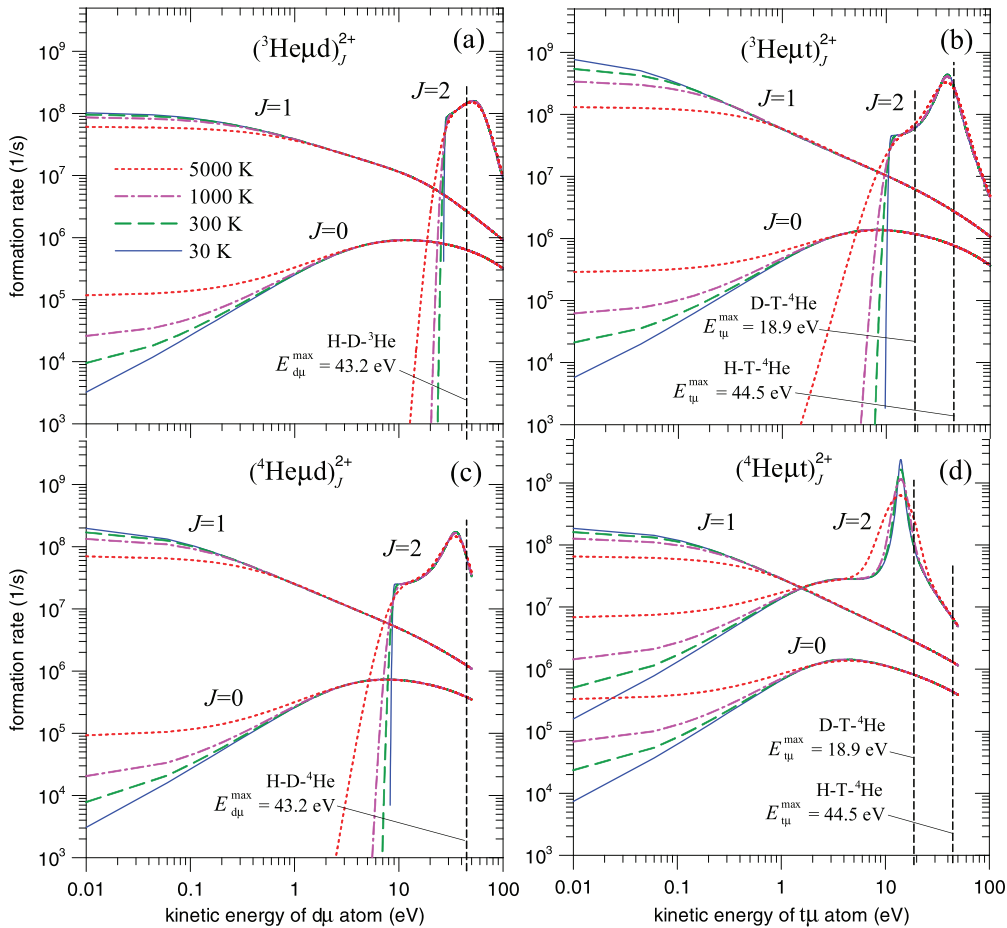
FIG. 5. (Color online) Average reaction rates (normalized to LHD) for the formation of $(\text{He}\mu h)_J^{2+}$ molecules in triple H-H'-He mixtures. Vertical dashed lines indicate maximal kinetic energies of $d\mu$ and $t\mu$ atoms formed due to muon transfer.

C. Average formation rates corresponding to H-H′-He gas mixtures

Average formation rates for the $(^{3,4}\text{He}\mu d)^{2+}_J$ and $(^{3,4}\text{He}\mu t)^{2+}_J$ molecules calculated according to Eq. (31) are presented in Fig. 5 as functions of kinetic energy of $d\mu$ and $t\mu$ atoms, for target temperatures $T = 30, 300, 1000$, and 5000 K. As expected, resonant peaks are shifted above the corresponding resonant collision energies (see Table I) and are also lower and wider with increasing temperature. The formation rates for molecules in the rotational state $J = 2$, $(^{3,4}\text{He}\mu d)^{2+}_2$ and $(^3\text{He}\mu t)^{2+}_2$, practically dominate above the energies corresponding to collision energy thresholds, whereas

the formation rate for the $(^4\text{He}\mu t)^{2+}_2$ molecule dominates above 1.5 eV (compare with Fig. 2 of the present paper and Fig. 2 of Ref. [33]). Below these energies, formation rates for $J = 1$ dominate. Kinetic energies gained by muonic atoms due to muon transfer (30), $E^{\max}_{h\mu}$, are indicated by vertical dashed lines. One can expect that in addition to molecules in the rotational state $J = 1$, molecules $(^{3,4}\text{He}\mu d)^{2+}_2$ and $(^{3,4}\text{He}\mu t)^{2+}_2$, whose formation is resonantly enhanced, will be effectively formed in the corresponding triple H-D-^{3,4}He and H(D)-T-^{3,4}He gas mixtures at all temperatures considered. This results from the fact that the energy domain of the resonant enhancement of the formation rate for each of these
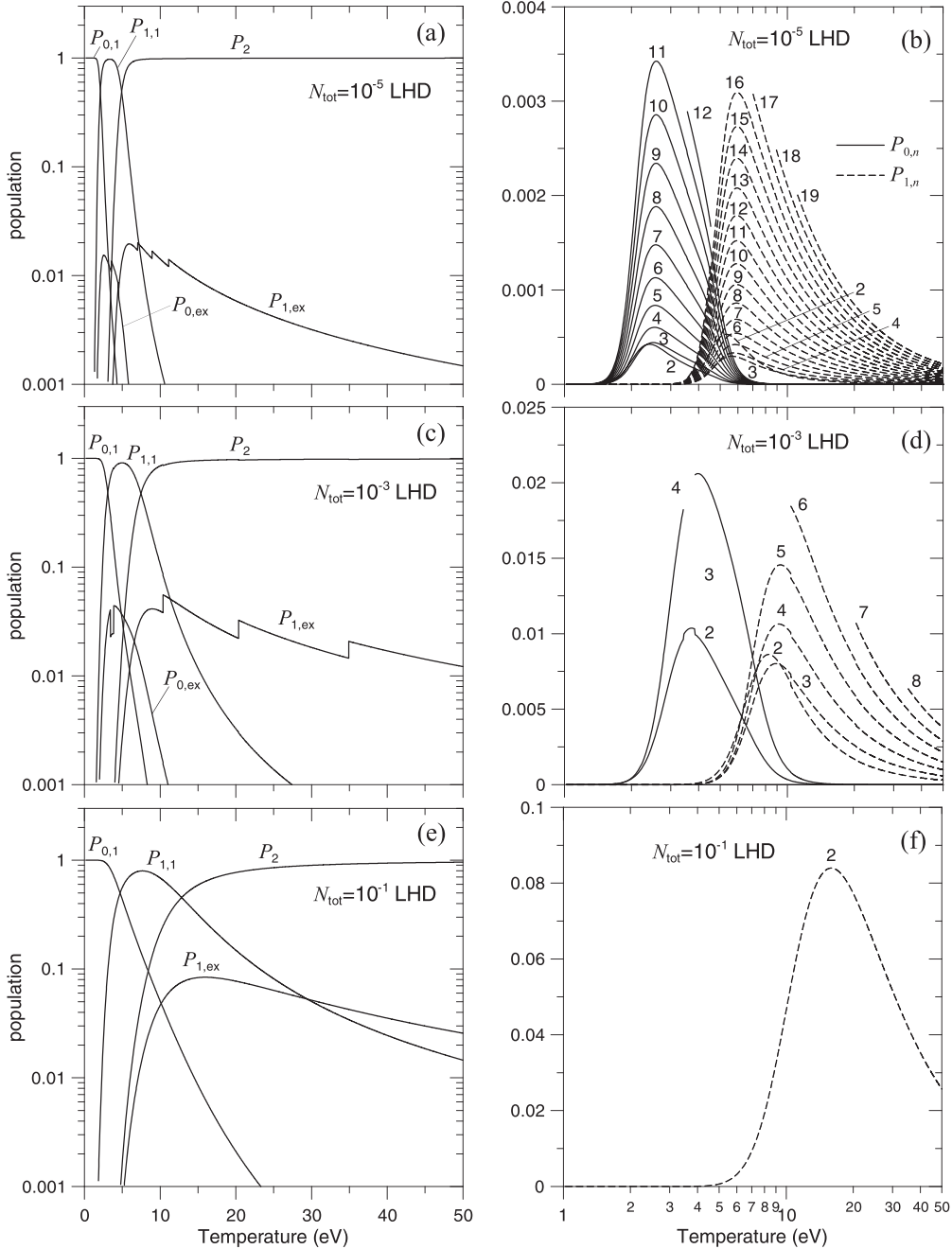
FIG. 7. Populations of the (a), (c), (e) ground state and (b), (d), (f) excited states of a helium atom and ion in H-He plasma, for $c_{\text{He}} = 0.5$ and N_{tot} indicated in figures. Total populations of excited states of helium atom ($P_{0,\text{ex}}$) and ion ($P_{1,\text{ex}}$) are presented in (a), (c), and (e).

molecules occupies a significant part of the corresponding energy range $(0, E_{h\mu}^{\max})$. The temperature dependence of the average formation rate in the vicinity of the resonant energy is mostly pronounced for the $({}^4\text{He}\mu t)_2^{2+}$ molecule [Fig. 5(d)]. The maximum value of the corresponding rate increases from 7.5×10^8 s^{-1} for $T = 5000$ K to 2.7×10^9 s^{-1} for $T = 30$ K. Formation rates for $J = 0$ are negligibly small at low energies when compared with those for $J = 1$. However, near the thresholds for the formation of $J = 2$ states, the formation rates for the $({}^{3,4}\text{He}\mu d)_0^{2+}$ and $({}^{3,4}\text{He}\mu t)_0^{2+}$ molecules are of the order of 10^6 s^{-1}, i.e., they are smaller than the corresponding rates for $J = 1$ [and 2 for $({}^4\text{He}\mu t)_0^{2+}$] by about one order of magnitude only. This fact may be important for experimental studies of nuclear fusion reactions occurring within these molecules. For example, the theoretically estimated fusion rate for the $({}^3\text{He}\mu d)_0^{2+}$ molecule, $\lambda_0^f \propto 10^5$ s$^{-1} - 10^6$ s^{-1} [24,55,56], is about three to four orders of magnitude greater than the fusion rate corresponding to the rotational state $J = 1$ of the molecule. In low-temperature binary mixtures, the rotational state $J = 1$ is mostly populated, thus, to be able to observe the fusion, a fast $J = 1 \rightarrow J = 0$ transition must occur. Experiments give an effective fusion rate, i.e., the rate averaged over populations of the rotational states. Therefore, λ_0^f can be obtained indirectly only; what is required is the precise value for the $1 \rightarrow 0$ transition. Mechanisms of this transition are, however, still hypothetical and the corresponding reaction rates were roughly estimated in [55,57]. Values of λ_0^f for $d - {}^3\text{He}$ fusion extracted from experimental data [58], $(4.5^{+2.6}_{-2.0}) \times 10^5$ s^{-1} and $(6.9^{+3.6}_{-3.0}) \times 10^5$ s^{-1}, for two densities of a D $- {}^3\text{He}$ mixture, $\varphi = 0.0585$ LHD and $\varphi = 0.168$ LHD, respectively, are subject to significant errors resulting from insufficient knowledge of the $1 \rightarrow 0$ transition rate. To clarify the situation and remove the existing ambiguities, more reliable data on the rotational transition is required. However, the accuracy of the experimental results should be improved in the H-D-^{3}He mixture, where an increased population of $({}^3\text{He}\mu d)_0^{2+}$ molecular states is expected.

D. Average formation rates corresponding to H-He plasma

The fraction of free electrons in H-He plasma, x_e, obtained by numerical solution of Eq. (35), is shown in Fig. 6 for plasma densities $N_{\text{tot}} = 10^{-5}$ LHD, 10^{-3} LHD, and 0.1 LHD, and for helium relative concentrations $c_{\text{He}} = 0.1$ and 0.5. Results corresponding to the same N_{tot} and different c_{He} are close at small temperatures and tend to zero for decreasing T. At the same time, results corresponding to the same c_{He} and different N_{tot} tend to the limit $1 + c_{\text{He}}$ for increasing T.
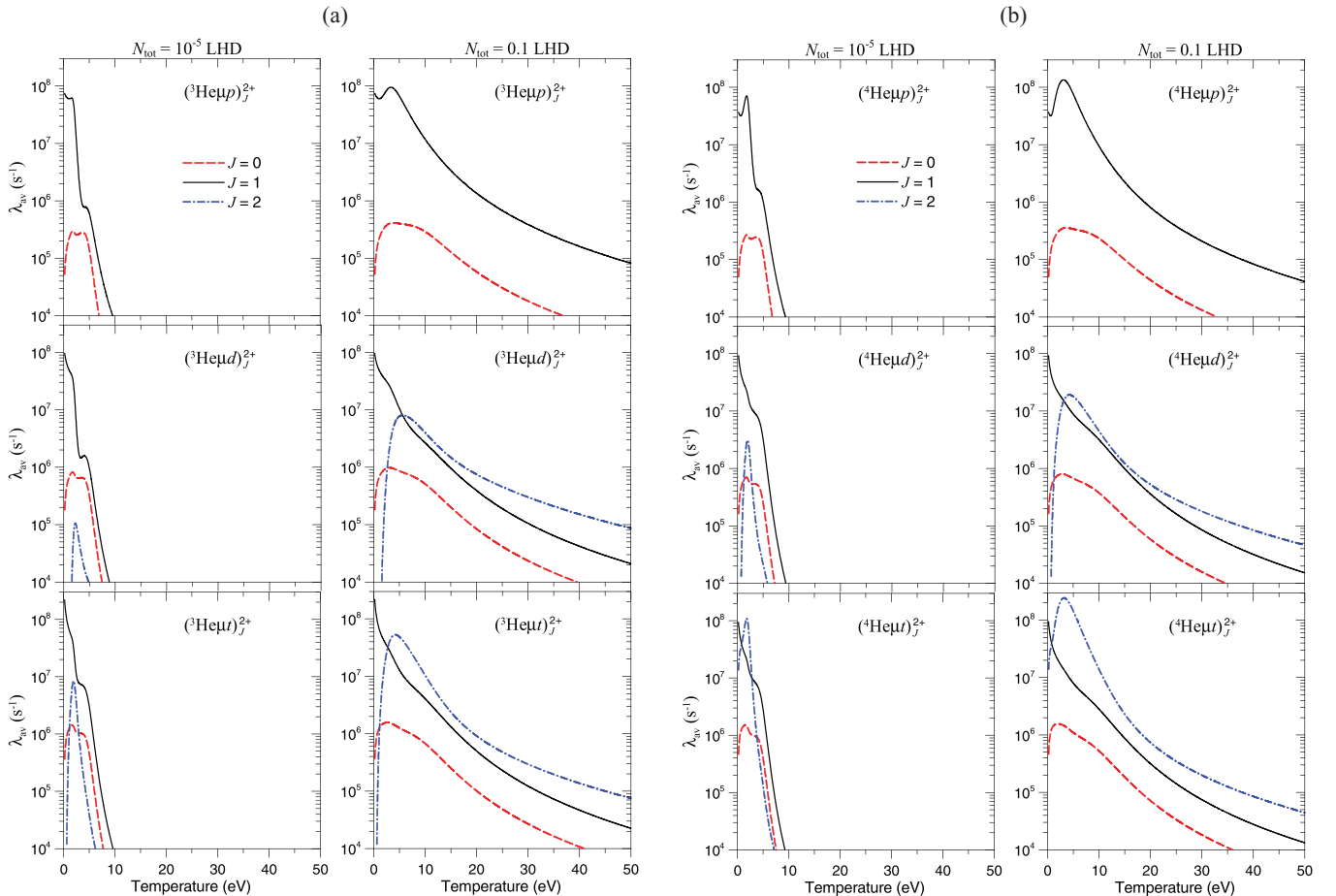
FIG. 8. (Color online) (a) Average reaction rates (normalized to LHD) for the formation of $({}^3\text{He}\mu h)_J^{++}$ molecules in H-He plasma, for plasma density $N_{\text{tot}} = 10^{-5}$ LHD (left column) and 0.1 LHD (right column), and for helium relative concentration $c_{\text{He}} = 0.5$ LHD. (b) The same as in (a), but for $({}^4\text{He}\mu h)_J^{++}$ molecules.

Both observations are in agreement with the corresponding temperature limits obtained in Sec. II B.

Populations $P_{r,n}$ calculated according to Eqs. (36)–(38) largely determine the temperature dependence of the average formation rates corresponding to H-He plasma. For a better understanding of the latter, $P_{r,n}$ are presented in the separate Fig. 7. Namely, $P_{r,1}$ corresponding to helium atom ($r = 0$) and ion ($r = 1$) as well as population P_2 (corresponding to He^{2+}) are presented for $c_{He} = 0.5$ in Figs. 7(a), 7(c), and 7(e) for $N_{tot} = 10^{-5}$ LHD, 10^{-3} LHD, 0.1 LHD, respectively. Populations $P_{r,n \geqslant 2}$ are presented in Figs. 7(b), 7(d), and 7(f). Total populations of excited helium atoms and ions defined as $P_{r,ex} = \sum_{n=2}^{n_r^{He}} P_{r,n}$ are also shown in Figs. 7(a), 7(c), and 7(e). It was proved by numerical calculation that all populations very weakly depend on helium relative concentration when $0.1 \leqslant c_{He} \leqslant 0.9$.

Average formation rates are calculated according to Eqs. (39). For $n > 10$, bare rates $\lambda_{0,n}(\varepsilon)$ (corresponding to collisions with singly excited helium atoms) are approximated by $\lambda_{0,10}(\varepsilon)$. This is justified by the fact that the rates $\lambda_{0,n>5}(\varepsilon)$ do not practically depend on n in the whole range of collision energy for molecules with $\varepsilon_J^b > I_1^{He}$ and above the collisional thresholds $I_1^{He} - \varepsilon_J^b$ for molecules with $\varepsilon_J^b < I_1^{He}$ (see Fig. 3). Below the thresholds, the contribution of $\lambda_{0,n>10}(\varepsilon)$ is irrelevant since $\lambda_{0,n}(\varepsilon)$ decrease with increasing n, and $\lambda_{0,10}(\varepsilon)$ is negligibly small. At the same time, $\lambda_{1,n>10}(\varepsilon)$ (corresponding to collisions with an excited helium ion) are neglected since $\lambda_{1,n}(\varepsilon)$ decrease with increasing n in the whole energy range considered, and $\lambda_{1,10}(\varepsilon)$ is negligibly small (see Fig. 4). The average formation rates are presented in Figs. 8(a) and 8(b) for $(^3He\mu h)_J^{2+}$ and $(^4He\mu h)_J^{2+}$, respectively, for two extreme plasma densities, $N_{tot} = 10^{-5}$ LHD (left column) and 0.1 LHD (right column), and helium relative concentration $c_{He} = 0.5$. Zero-temperature limits of the rates corresponding to rotational states $J = 0$ and 1 of all molecules, as well as for the $(^4He\mu t)_2^{2+}$ molecule, i.e., for molecules characterized by $\varepsilon_2^b > I_0^{He} = 24.6$ eV, do not practically depend on plasma density and are equal to zero-energy limits of the corresponding bare rates for transitions induced by collisions with the ground-state helium atoms (Fig. 2). This is due to the fact that for all plasma densities, the population of helium atoms in the ground state is $P_{0,1} = 1$ for $T \to 0$ (see Fig. 7). As a consequence, one obtains, from Eqs. (39), $\lambda_{av} = \lambda_{0,1}^{Maxw.} = \lambda_{0,1}(0)$. At the same time, reaction rates for the formation of the remaining molecules in the rotational state $J = 2$ (characterized by $\varepsilon_2^b < I_0^{He} = 24.6$ eV) reach values that tend to zero at low temperatures. This is because formation of the molecules proceeds either on excited helium atoms and ions at slow collisions, or on the ground-state ones at energies exceeding the corresponding energy thresholds $I_0^{He} - \varepsilon_2^b$. Therefore, the rates vanish due to vanishing populations of the excited atoms and ions at $T \to 0$ in the first case (see Fig. 7), or due to vanishing bare formation rates below the thresholds in the second case.

According to Figs. 7(a), 7(c), and 7(e), it can be stated (without taking into account the population of He^{2+} ions, P_2) that populations of the ground-state helium atoms ($P_{0,1}$) and ions ($P_{1,1}$) dominate at plasma temperatures below 7, 12, and 30 eV, respectively. The populations decrease rapidly with increasing T (e.g., for $N_{tot} = 10^{-5}$ LHD, $P_{0,1}$ decreases
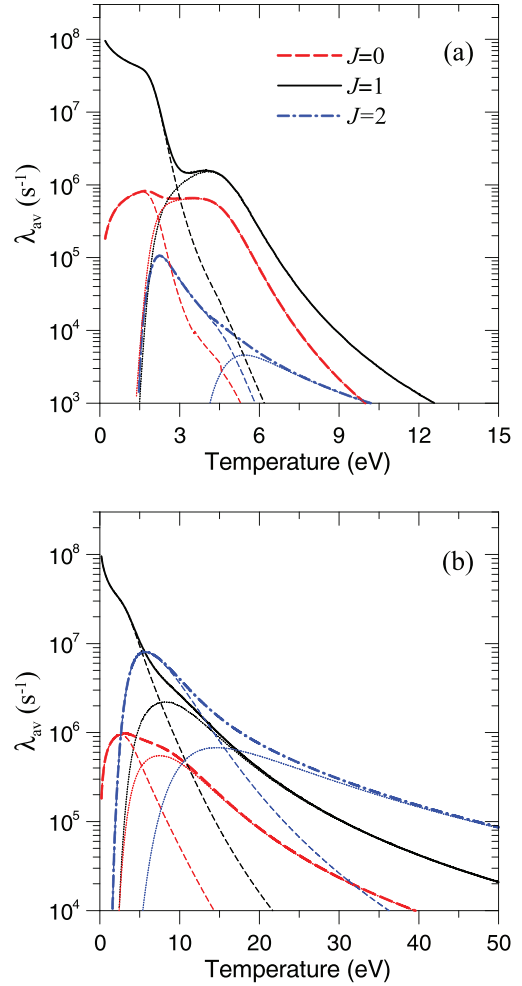
FIG. 9. (Color online) Contribution of helium atoms (short-dashed line) and ions (dotted line) to the average formation rates for the $(^3He\mu d)_J^{2+}$ molecule for $c_{He} = 0.5$ and two plasma concentrations: (a) 10^{-5} LHD and (b) 0.1 LHD.

rapidly above 2 eV and $P_{1,1}$ above 5 eV); however, the decrease becomes milder with increasing N_{tot}. As a consequence, the average formation rates presented in Fig. 8 exhibit a similar temperature and density behavior. For similar reasons, this effect occurs also at higher temperatures, where collisions with excited helium atoms and ions dominate. The increase of λ_{av} with increasing N_{tot} is particularly evident for reaction rates corresponding to $J = 2$.

The average formation rates for $J = 1$ dominate for all plasma densities at low temperatures, whereas for $(^{3,4}He\mu p)_1^{2+}$ molecules, it dominates in the whole temperature range. This is a consequence of an analogous behavior of the corresponding bare formation rates as functions of collision energy (see Fig. 2). At the same time, $(^4He\mu t)_2^{2+}$ is the only molecule whose formation rate for $N_{tot} = 10^{-5}$ LHD exceeds the corresponding formation rate for $J = 1$. This is due to the existence of strong resonance in $(t\mu)_{1s} + {}^4He^{2+}$ scattering at collision energy 7.9 eV [Fig. 2(d)]. Resonantly enhanced formation of $(^{3,4}He\mu d)_2^{2+}$ and $(^{3,4}He\mu t)_2^{2+}$ molecules in H-He plasma dominates for $T > 5$ eV and $T > 3$ eV, respectively, at plasma density 0.1 LHD, whereas the formation of $(^{3,4}He\mu p)_1^{2+}$
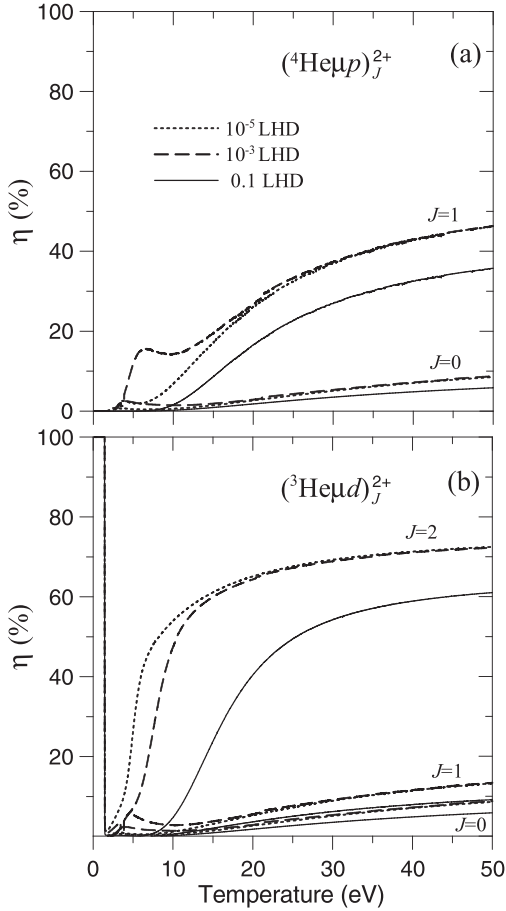
FIG. 10. Relative contribution of excited states of helium atoms and ions to the average reaction rate for the formation of the (a) $(^4\text{He}\mu p)_J^{++}$ and (b) $(^3\text{He}\mu d)_J^{++}$ molecule in H-He plasma, for $c_{\text{He}} = 0.5$ and different plasma concentrations.

molecules dominates in a wide range of plasma temperature ($T \leqslant 50$ eV) and density (10^{-5}–0.1 LHD). However, the most interesting conclusion resulting from Figs. 8(a) and 8(b) is that in some regions of temperature, the average formation rates for $(^{3,4}\text{He}\mu d)_0^{2+}$ and $(^{3,4}\text{He}\mu t)_0^{2+}$ molecules are smaller than the corresponding rates for $J = 1$ (10^{-5} LHD) and $J = 1,2$ (0.1 LHD) by at most one order of magnitude.

The average formation rates, $\lambda_{\text{av},r} = \sum_{n=1}^{n_r^{\text{He}}} P_{r,n}^{\text{He}} \lambda_{r,n}^{\text{Maxw.}}$, corresponding to collisions with helium atoms ($r = 0$) and ions ($r = 0$), are presented in Fig. 9 for $(^3\text{He}\mu d)_{0,1,2}^{2+}$ molecular states, as examples. For plasma density $N_{\text{tot}} = 10^{-5}$ LHD, formation induced by collisions with helium atoms (in the ground and excited states) dominates for rotational states $J = 0, 1$, and 2 at temperatures below 2, 3, and 5 eV, respectively. For plasma density 0.1 LHD, the corresponding temperatures are 5, 8, and 16 eV. Above these temperatures, formation induced by collisions with helium ions (in the ground and excited states) dominates. To illustrate the role of excited states of helium atoms and ions in the formation processes, the parameter $\eta = \lambda_{\text{av,ex}}/\lambda_{\text{av}}$, where $\lambda_{\text{av,ex}} = \lambda_{\text{av}} - \sum_{r=0}^{1} P_{r,1}^{\text{He}} \lambda_{r,1}^{\text{Maxw.}}$, is presented for $c_{\text{He}} = 0.5$ and three plasma concentrations ($N_{\text{tot}} = 10^{-5}$, 10^{-3}, and 0.1 LHD) in Figs. 10(a) and 10(b) for $(^4\text{He}\mu p)_{0,1}^{2+}$ and $(^3\text{He}\mu d)_{0,1,2}^{2+}$, respectively. As is seen from the figures, η

increases with decreasing N_{tot} and increasing J (i.e., decreasing binding energy). For $T = 50$ eV, η receives about $35-43\%$ and $61-72\%$ for $(^4\text{He}\mu p)_1^{2+}$ and $(^3\text{He}\mu d)_2^{2+}$, respectively. For the latter molecule, η receives even 100% below 2 eV for all plasma concentrations considered. This is caused by the small value of binding energy of the molecule (7.25 eV), which formation proceeds mainly due to collision with an excited helium atom or ion. However, according to Fig. 8(a), the corresponding average formation rate is negligibly small below 2 eV.

IV. SUMMARY AND CONCLUSIONS

The reaction rates for the Auger formation of $(\text{He}\mu h)_J^{2+}$ molecules, where $h = p, d, t$ and $\text{He} = ^{3,4}\text{He}$, in collisions of $(h\mu)_{1s}$ atoms with helium atoms and ions in the ground and singly excited states ($n \leqslant 10$) were calculated for all rotational states of the molecules ($J = 0,1,2$) in the energy range 0.1–50 eV. Results were obtained using a one-level adiabatic approximation for the description of the three-body system He^{2+}-μ-h in the $2p\sigma$ state and the dipole approximation for interaction of the system with helium electrons. The latter were described using an independent-particle model. All partial waves of relative $(h\mu)_{1s} + \text{He}^{2+}$ motion contributing to the formation process were included. It was found that shape resonances corresponding to the partial d wave (for $h = p$) and f wave (for $h = d, t$) significantly enhance the formation rates for $J = 1$ and $J = 2$, respectively. The rates (normalized to the liquid hydrogen density) corresponding to collisions of $(h\mu)_{1s}$ with the ground-state helium atoms reach maximum values of the order of 10^8-10^9 s^{-1} and are several times greater than their excited-state counterparts. The latter very weakly depend on n for all collision energies considered if binding energies of the molecules exceed the ionization potential of the helium ion ($\varepsilon_J^b > 54.4$ eV). For molecules with $\varepsilon_J^b < 54.4$ eV, the rates very weakly depend on n for collision energies exceeding the thresholds $I_1^{\text{He}} - \varepsilon_J^b$, whereas below the thresholds, they significantly decrease with increasing n. The formations rates corresponding to collisions with excited helium ions with $n = 2$ are at least one order of magnitude smaller than their ground-state counterparts and decrease with increasing n in the whole range of energy considered.

Using the above results, the average formation rates corresponding to triple H-H′-He gas mixtures (H and H′ are different hydrogen isotopes) at several temperatures between 30 and 5000 K, as well as hydrogen-helium plasma at temperature $T \leqslant 50$ eV, were calculated. It was found that resonantly enhanced formation of the molecules in the rotational state $J = 2$, $(^{3,4}\text{He}\mu d)_2^{2+}$ and $(^{3,4}\text{He}\mu t)_2^{2+}$, dominates in the corresponding H-D-^{3,4}He and H(D)-T-^{3,4}He mixtures for kinetic energy of $(d\mu)_{1s}$ and $(t\mu)_{1s}$ atoms greater than 10 eV. The atoms obtain such a high kinetic energy due to the ground-state muon transfer from lighter to heavier hydrogen isotope. It is expected that thermalization of the resulting muonic atoms in H-D-He and H-T-He mixtures, in which hydrogen is the dominant component, is suppressed due to a strong Ramsauer-Townsend effect in $d\mu + \text{H}_2$ and $t\mu + \text{H}_2$ collisions [36,47]. However, Monte Carlo simulations are necessary to draw a final conclusion. It was found that the resonantly enhanced formation of $(^{3,4}\text{He}\mu d)_2^{2+}$ and $(^{3,4}\text{He}\mu t)_2^{2+}$ molecules in H-He

plasma dominates for $T > 5$ eV and $T > 3$ eV, respectively, at plasma density of 0.1 LHD, whereas the formation of $(^{3,4}\text{He}\mu p)_1^{2+}$ molecules dominates in a wide range of plasma temperatures ($T \leqslant 50$ eV) and density ($10^{-5}-0.1$ LHD).

Molecules in the rotational ground state $J = 0$, $(^{3,4}\text{He}\mu d)_0^{2+}$ and $(^{3,4}\text{He}\mu t)_0^{2+}$, can be directly formed in triple H-H′-He gas mixtures as well as in H-He plasma. The corresponding formation rates are [in certain areas of kinetic energy of muonic hydrogen isotopes (H-H′-He mixtures) or temperatures (H-He plasma)] only one order of magnitude smaller than the rates for the formation of the molecules in excited states $J = 1$ and 2. This fact may be important for the experimental study of nuclear synthesis reactions occurring within these molecules.

The above results provide an extension of Auger formation rates corresponding to collisions of muonic hydrogen isotopes with the ground-state helium atoms, presented in Refs. [20,29,30] for the rotational state of the resulting muonic molecules $J = 1$, and in Ref. [33] for the $(^{4}\text{He}\mu p)_1^{2+}$ and $(^{3}\text{He}\mu d)_{0,1,2}^{2+}$ molecules.

ACKNOWLEDGMENTS

[1] K. Nagamine, *Introductory Muon Science* (Cambridge University Press, Cambridge, UK, 2003).

[2] K. Ishida, K. Nagamine, T. Matsuzaki, and N. Kawamura, J. Phys. G **29**, 2043 (2003); L. Bracci and G. Fiorentini, Phys. Rep. **86**, 169 (1982); A. Guła, Acta. Phys. Pol. B **16**, 589 (1985).

[3] K. Nagamine and M. Kamimura, in *Advances in Nuclear Physics*, edited by J. W. Negele and E. W. Vogt, Vol. 24 (Plenum Press, NY, 1998), p. 151.

[4] P. Froelich, Adv. Phys. **41**, 405 (1992).

[5] H. E. Rafelski, D. Harley, G. R. Shin, and J. Rafelski, J. Phys. B **24**, 1469 (1991).

[6] W. H. Breunlich, P. Kammel, J. S. Cohen, and M. Leon, Annu. Rev. Nucl. Part. Sci. **39**, 311 (1989).

[7] S. S. Gerstein, Yu. V. Petrov, and L. I. Ponomarev, Sov. Phys. Usp. **33**, 591 (1990); L. I. Ponomarev, Contemp. Phys. **31**, 219 (1990).

[8] D. Harley, B. Mueller, and J. Rafelski, J. Phys. G **16**, 281 (1990).

[9] V. B. Belyaev, S. A. Rakityansky, H. Fiedeldey, and S. A. Sofianos, Phys. Rev. A **50**, 305 (1994); J. L. Friar, B. F. Gibson, H. C. Jean, and G. L. Payne, Phys. Rev. Lett. **66**, 1827 (1991).

[10] C. Rolfs, Prog. Part. Nucl. Phys. **46**, 23 (2001); C. Rolfs, H. P. Trautvetter, and W. S. Rodney, Rep. Prog. Phys. **50**, 233 (1987); V. B. Belyaev, M. Decker, H. Fiedeldey, S. A. Rakityansky, W. Sandhas, and S. A. Sofianos, Nukleonika **40**, 3 (1995).

[11] D. F. Measday, Phys. Rep. **354**, 243 (2001); A. Bertin and A. Vitale, in *Fifty Years of Weak-Interaction Physics*, edited by A. Bertin, R. A. Ricci, and A. Vitale (Italian Physical Society, Bologna, 1984); N. C. Mukhopadhyay, Phys. Rep. **30**, 1 (1977); E. Zavattini, in *Muon Physics II*, edited by V. W. Hughes and C. S. Wu (Academic, New York, 1975), p. 219; V. M. Bystritsky *et al.*, Phys. Rev. A **69**, 012712 (2004).

[12] V. A. Andreev *et al.*, Phys. Rev. Lett. **110**, 012504 (2013); **99**, 032002 (2007).

[13] P. Kammel, Nucl. Phys. A **844**, 181c (2010).

[14] P. Ackerbauer *et al.*, Phys. Lett. B **417**, 224 (1998).

[15] J. M. Dong *et al.*, Phys. Lett. B **704**, 600 (2011).

[16] P. Strasser *et al.*, Nucl. Phys. B (Proc. Suppl.) **149**, 390 (2005).

[17] D. G. Fleming *et al.*, Science **331**, 448 (2011).

[18] R. Pohl *et al.*, Nature (London) **466**, 213 (2010).

[19] R. G. Newton, *Scattering Theory of Waves and Particles* (Springer, New York, 1982).

[20] Yu. A. Aristov, A. V. Kravtsov, N. P. Popov, G. E. Solyakin, N. F. Truskova, and M. P. Fajfman, Yad. Fiz. **33**, 1066 (1981) [Sov. J. Nucl. Phys. **33**, 564 (1981)].

[21] V. B. Belyaev, O. I. Kartavtsev, V. I. Kochkin, and E. A. Kolganova, Z. Phys. D **41**, 239 (1997); Phys. Rev. A **52**, 1765 (1995).

[22] A. V. Kravtsov, A. I. Mikhailov, and V. I. Savichev, Hyperfine Interact. **82**, 205 (1993).

[23] J. Gronowski, W. Czapliński, and N. Popov, Acta Phys. Pol. A **106**, 795 (2004).

[24] Z. Kino and M. Kamimura, Hyperfine Interact. **82**, 195 (1993).

[25] J. Wallenius and P. Froelich, Hyperfine Interact. **118**, 223 (1999).

[26] D. I. Abramov and V. V. Gusev, J. Phys. B **33**, 891 (2000).

[27] O. I. Kartavtsev, V. I. Kochkin, and E. A. Kolganova, Hyperfine Interact. **118**, 235 (1999).

[28] V. I. Korobov, Hyperfine Interact. **101/102**, 329 (1996).

[29] A. V. Kravtsov, A. I. Mikhailov, and N. P. Popov, J. Phys. B **19**, 2579 (1986).

[30] A. V. Kravtsov, A. I. Mikhailov, and N. P. Popov, J. Phys. B **19**, 1323 (1986); V. K. Ivanov, A. V. Kravtsov, A. I. Mikhailov, N. P. Popov, and V. I. Fomichev, Zh. Eksp. Teor. Fiz. **91**, 358 (1986) [Sov. Phys. JETP **64**, 210 (1986)].

[31] S. S. Gerstein, Zh. Eksp. Teor. Fiz. **43**, 706 (1962) [Sov. Phys. JETP **16**, 501 (1963)]; A. V. Matveenko and L. I. Ponomarev, Zh. Eksp. Teor. Fiz. **63**, 48 (1972) [Sov. Phys. JETP **36**, 24 (1973)].

[32] V. M. Bystritsky *et al.*, Zh. Eksp. Teor. Fiz. **84**, 1257 (1983) [Sov. Phys. JETP **57**, 728 (1983)]; T. Matsuzaki, K. Ishida, K. Nagamine, Y. Hirata, and R. Kadono, Muon Catalyzed Fusion **2**, 217 (1988); A. J. Cafrey *et al.*, *ibid.* **1**, 53 (1987); R. Jacot-Guillarmod *et al.*, Phys. Rev. A **38**, 6151 (1988); K. Ishida *et al.*, Hyperfine Interact. **82**, 111 (1993); S. Tresch *et al.*, Phys. Rev. A **57**, 2496 (1998); **58**, 3528 (1998); B. Gartner *et al.*,

ibid. **62**, 012501 (2000); E. M. Maev *et al.*, Hyperfine Interact. **119**, 121 (1999); M. Augsburger *et al.*, Phys. Rev. A **68**, 022712 (2003).

[33] W. Czapliński, J. Gronowski, W. Kamiński, and N. Popov, Phys. Lett. A **375**, 155 (2010).

[34] L. I. Ponomarev and M. P. Faifman, Zh. Eksp. Teor. Fiz. **71**, 1689 (1976) [Sov. Phys. JETP **44**, 886 (1976)].

[35] L. I. Ponomarev, I. V. Puzynin, and T. P. Puzynina, J. Comp. Phys. **22**, 125 (1976).

[36] D. I. Abramov, V. V. Gusev, and L. I. Ponomarev, Phys. Atom. Nucl. **64**, 1364 (2001); C. Chiccoli *et al.*, Muon Catalyzed Fusion **7**, 87 (1992); A. Adamczak *et al.*, At. Data Nucl. Data Tables **62**, 255 (1996).

[37] L. I. Ponomarev, S. I. Vinitsky, and F. R. Vukajlović, J. Phys. B **13**, 847 (1980); S. I. Vinitsky and L. I. Ponomarev, Fiz. Elem. Chastits At. Yadra **13**, 1336 (1982) [Sov. J. Part. Nucl. **13**, 557 (1982)].

[38] L. D. Landau and E. M. Lifshitz, *Quantum Mechanics: Non-relativistic Theory* (Pergamon, New York, 1977).

[39] H. A. Bethe and E. E. Salpeter, *Quantum Mechanics of One- and Two-electron Atoms* (Plenum, New York, 1987).

[40] B. H. Bransden and C. J. Joachain, *Physics of Atoms and Molecules* (Prentice Hall, Englewood Cliffs, NJ, 2003).

[41] R. L. Brown, Phys. Rev. A **1**, 341 (1970).

[42] R. Edmonds, *Angular Momentum in Quantum Mechanics* (Princeton University Press, Princeton, NJ, 1996).

[43] V. E. Markushin, Phys. Rev. A **50**, 1137 (1994).

[44] J. S. Cohen, Phys. Rev. A **34**, 2719 (1986); L. I. Menshikov, Muon Catalyzed Fusion **2**, 173 (1988).

[45] D. J. Abott *et al.*, Phys. Rev. A **55**, 214 (1997); M. Jeitler *et al.*, *ibid.* **51**, 2881 (1995).

[46] S. Y. Khalantari and V. Tahani, Hyperfine Interact. **142**, 627 (2002); A. Adamczak, *ibid.* **101/102**, 113 (1996).

[47] F. Mulhauser *et al.*, Phys. Rev. A **73**, 034501 (2006).

[48] M. P. Faifman, L. I. Menshikov, and T. A. Strizh, Muon Catal. Fusion **4**, 1 (1989).

[49] L. D. Landau and E. M. Lifshitz, *Statistical Physics* (Pergamon, London, 1963).

[50] L. I. Men'shikov and L. N. Somov, Sov. Phys. Usp. **33**, 616 (1990).

[51] H. R. Griem, *Principles of Plasma Spectroscopy* (Cambridge University Press, Cambridge, UK, 1997).

[52] R. Kippenhahn and A. Weigert, *Stellar Structure and Evolution* (Springer, New York, 1994); J. P. Cox and R. T. Giuli, *Principles of Stellar Structure* (Gordon and Breach, New York, 1968), Vol. 1.

[53] H. Bradt, *Astrophysics Processes* (Cambridge University Press, Cambridge, UK, 2008), Chap. 4 Supplement, http://www.cambridge.org/us/files/5413/6681/8627/7706_Saha_equation.pdf; H. F. Nelson, J. Spacecr. Rockets **9**, 177 (1972).

[54] C. W. Allen, *Astrophysical Quantities* (Athlone, London, 1973).

[55] L. N. Bogdanova, V. I. Korobov, and L. I. Ponomarev, Hyperfine Interact. **118**, 3 (1999).

[56] W. Czapliński, A. V. Kravtsov, A. I. Mikhailov, and N. Popov, Phys. Lett. A **219**, 86 (1996); Eur. Phys. J. D **3**, 223 (1998); F. M. Pen'kov, Yad. Fiz. **60**, 1003 (1997) [Phys. Atom. Nucl. **60**, 897 (1997)]; V. B. Belyaev, V. I. Korobov, and S. A. Rakityansky, Few-Body Syst. **17**, 243 (1994).

[57] W. Czapliński, J. Gronowski, N. Popov, and M. Zegrodnik, J. Phys. B **41**, 65202 (2008); W. Czapliński, J. Gronowski, and N. Popov, J. Phys. B **41**, 035101 (2008); W. Czapliński, E. Guła, and N. Popov, Kerntechnik **67**, 290 (2002); W. Czapliński, A. I. Mikhailov, and I. A. Mikhailov, Hyperfine Interact. **142**, 577 (2002); W. Czapliński, M. Filipowicz, E. Gula, A. V. Kravtsov, A. I. Mikhailov, and N. Popov, Z. Phys. D **37**, 283 (1996).

[58] V. M. Bystritsky *et al.*, Eur. Phys. J. D **38**, 455 (2006).